

UNIVERSIDADE FEDERAL DE MINAS GERAIS  
Programa de Pós-Graduação em Engenharia Metalúrgica, Materiais e de Minas

Tese de Doutorado

“Síntese otimizada e funcionalização de redes tridimensionais organometálicas  
(MOFs) para adsorção de gases”

Autor: Aline Geice Vitor Silva  
Orientador: Prof. Dr. Wander Luiz Vasconcelos  
Coorientador: Dr. Peter George Weidler

Aline Geice Vitor Silva

“Síntese otimizada e funcionalização de redes tridimensionais organometálicas (MOFs) para adsorção de gases”

“Optimized synthesis and functionalization of metal-organic frameworks (MOFs) for gas adsorption”

Tese apresentada ao Programa de Pós-Graduação em Engenharia Metalúrgica, Materiais e de Minas da Universidade Federal de Minas Gerais, como requisito parcial para obtenção do Grau de Doutora em Engenharia Metalúrgica, de Materiais e de Minas.

Área de Concentração: Ciência e Eng. Materiais

Orientador: Prof. Dr. Wander Luiz Vasconcelos

Coorientador: Dr. Peter George Weidler

Belo Horizonte

Universidade Federal de Minas Gerais

Escola de Engenharia

2020

S586s	<p>Silva, Aline Geice Vitor.          Síntese otimizada e funcionalização de redes tridimensionais organometálicas (MOFs) para adsorção de gases [recurso eletrônico] = Optimized synthesis and functionalization of metal-organic frameworks (MOFs) for gas adsorption / Aline Geice Vitor Silva. – 2020.          1 recurso online (xiii, 68 f. : il., color.) : pdf.</p> <p>Orientador: Wander Luiz Vasconcelos.          Coorientador: Peter George Weidler.</p> <p>Tese (doutorado) - Universidade Federal de Minas Gerais, Escola de Engenharia.</p> <p>Bibliografia: f. 59-68.</p> <p>Exigências do sistema: Adobe Acrobat Reader.</p> <p>1. Engenharia Metalúrgica - Teses. 2. Adsorção - Teses.          I. Vasconcelos, Wander Luiz. II. Weidler, Peter George.          III. Universidade Federal de Minas Gerais. Escola de Engenharia.          IV. Título.</p>
	CDU: 669(043)

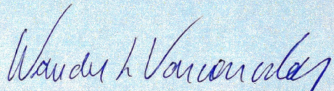


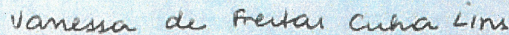


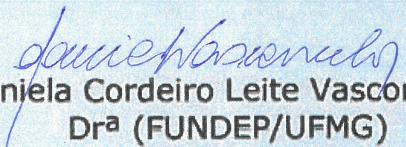
**UNIVERSIDADE FEDERAL DE MINAS GERAIS**  
**ESCOLA DE ENGENHARIA**  
Programa de Pós-Graduação em Engenharia  
Metalúrgica, Materiais e de Minas

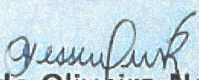


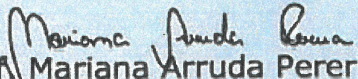
Tese intitulada "**Síntese Otimizada e Funcionalização de Redes Tridimensionais Organometálicas (mofs) para Adsorção de Gases**", área de concentração: Ciência e Engenharia de Materiais, apresentada pela candidata **Aline Geice Vitor Silva**, para obtenção do grau de Doutora em Engenharia Metalúrgica, Materiais e de Minas, aprovada pela comissão examinadora constituída pelos seguintes membros:

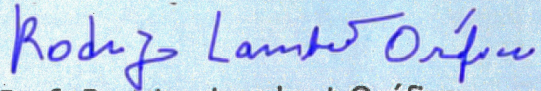
  
Prof. Wander Luiz Vasconcelos  
Orientador - PhD (UFMG)

  
Prof<sup>a</sup> Vanessa de Freitas Cunha Lins  
Dr<sup>a</sup> (UFMG)

  
Daniela Cordeiro Leite Vasconcelos  
Dr<sup>a</sup> (FUNDEP/UFMG)

  
Prof<sup>a</sup> Jéssica de Oliveira Nótório Ribeiro  
Dr<sup>a</sup> (UFLA)

  
Prof<sup>a</sup> Mariana Arruda Pereria  
Dr<sup>a</sup> (UFSJ)

  
Prof. Rodrigo Lambert Oréfice  
Coordenador do Programa de Pós-Graduação em Engenharia  
Metalúrgica, Materiais e de Minas/UFMG

Belo Horizonte, 30 de março de 2020



## AGRADECIMENTOS

Agradeço a Deus por me guiar e colocar oportunidades grandiosas em minha vida. Aos meus pais, Lúcia e Alípio, meus irmãos Danielle e Michel e aos meus avós Terezinha e Miguel por entender os momentos de ausência, pelo apoio e por sempre acreditar nos meus sonhos. Aos orientadores Dr. Wander Vasconcelos, Dr. Peter Weidler e Dra. Daniela Vasconcelos pelo incentivo, direção e confiança em todos os momentos. Aos alunos de iniciação científica Danielle, João e Nicolas pelo auxílio, pelas boas conversas e pelas trocas de experiências. Às equipes dos *Laboratórios de Materiais Cerâmicos (LMC)* e *Institut für Funktionelle Grenzflächen (IFG/KIT)* pelos ensinamentos transferidos e pela amizade. Ao CNPq, ao PROEX-CAPES e à UFMG pelo suporte financeiro durante essa pesquisa. Aos amigos pelos momentos de aprendizado e diversão que passamos juntos.

“Faça tudo da forma mais simples possível, mas não simplista.”  
*[Man muß die Dinge so einfach wie möglich machen. Aber nicht einfacher.]*

Albert Einstein



## RESUMO

As estruturas metalorgânicas (MOFs) receberam intenso interesse na última década devido à sua ampla aplicação. A MOF mais produzida no mundo é a HKUST-1 ou  $\text{Cu}_3(\text{BTC})_2$ , formada por nós metálicos de cobre e pelo ligante ácido 1,3,5-benzentricarboxílico (BTC). Com vasta aplicação industrial, favorece o desenvolvimento de rotas alternativas para sua fabricação, além do aprimoramento de métodos existentes devido ao surgimento recente dessas estruturas. Algumas falhas encontradas nos procedimentos de obtenção de MOFs incluem tempo de preparo, utilização de reagentes não ambientalmente amigáveis e, para o caso de filmes finos metalorgânicos (SURMOFs), a possibilidade de deposição em diferentes superfícies. Assim, o propósito desta tese foi investigar os métodos de obtenção de MOFs como filmes finos e MOFs particulados, visando encontrar rotas mais simples para orientar o crescimento das estruturas metalorgânicas em substratos de sílica, otimizar o tempo de obtenção de MOFs particulados, e encontrar alternativas sustentáveis ao uso de solventes orgânicos durante o processo. Os resultados dessa investigação incluem a formação pela primeira vez de SURMOFs pelo método *spray layer-by-layer* com orientação preferencial na direção [222] sobre a superfície de sílica SBA-15 ativada, confirmada por difração de raios-X (DRX) e a construção da MOF corroborada pelas bandas  $1652\text{ cm}^{-1}$  and  $1384\text{ cm}^{-1}$  características dos grupos C=O presentes no ligante precursor (BTC) obtidas por infravermelho com transformada de Fourier (FTIR). Esse estudo também mostrou que a utilização de irradiação ultrassom com energia localizada por baixíssimo tempo (1 min e 5 min) durante o processo de síntese permite a formação de Cu-BTC com alto rendimento de 78,1%, baseado na quantidade de cobre. As estruturas obtidas se mostraram alongadas, com formação inédita de bastão com tamanhos de 1–2  $\mu\text{m}$ . Esses resultados foram comprovados por DRX, FTIR, microscopia eletrônica de varredura (MEV) e microscopia eletrônica de transmissão (MET). Enquanto a maioria das metodologias emprega solventes orgânicos, este trabalho também avaliou com sucesso a possibilidade de utilizar água para a fabricação de MOFs em diferentes

proporções metal-ligante (Cu:BTC 1,8:1 e 1:1), buscando a formação de estruturas metalorgânicas altamente organizadas. Além de sintetizadas em ambiente aquoso, essas MOFs apresentaram capacidade de captura de dióxido de carbono, e contribui para o desenvolvimento de materiais sustentáveis. Em resumo, os resultados do estudo e modificação dos métodos colaborou significativamente para o aprimoramento das sínteses de MOF e suas aplicações.

Palavras-chaves: estruturas metalorgânicas (MOFs), monocamada automontada (SAM), funcionalização de sílica, morfologia, dióxido de carbono, ciclos de adsorção e dessorção



## ABSTRACT

Metal-organic frameworks (MOFs) have received intense interest in the last decade due to their wide application. The most produced MOF in the world is HKUST-1 or  $\text{Cu}_3(\text{BTC})_2$ , formed by copper metallic clusters and by 1,3,5-benzentricarboxylic acid ligand (BTC). With a wide industrial application, it favors the development of alternative routes for its manufacture, in addition to the improvement of existing methods due to the recent appearance of these structures. Some failures found in the procedures for obtaining MOFs include preparation time, use of environmentally friendly reagents and, in the case of thin metal-organic films (SURMOFs), the possibility of deposition on different surfaces. Thus, the purpose of this thesis was to investigate methods of obtaining MOFs such as thin films and particulate MOFs, in order to find simpler routes to guide the growth of metal-organic frameworks on silica substrates, optimize the time to obtain particulate MOFs, and find sustainable alternatives to the use of organic solvents during the process. The results of this investigation include the first time formation of SURMOFs by the spray layer-by-layer method with preferential orientation in the direction [222] on the activated SBA-15 silica surface, confirmed by X-ray diffraction (XRD) and corroborated of MOF building by bands  $1652\text{ cm}^{-1}$  and  $1384\text{ cm}^{-1}$  characteristic of groups  $\text{C}=\text{O}$  present in the precursor ligand (BTC) obtained by infrared with Fourier transform (FTIR). This study also showed the use of ultrasound irradiation with localized energy for a very short time (1 min and 5 min) during the synthesis process allows the formation of Cu-BTC with a high yield of 78.1%, based on copper. The obtained structures were shown to be elongated, with an unprecedented formation of rods with sizes of 1–2  $\mu\text{m}$ . These results were confirmed by XRD, FTIR, scanning electron microscopy (SEM) and transmission electron microscopy (MET). While most methodologies use organic solvents, this work has also successfully evaluated the possibility of using water for the manufacture of MOFs in different metal-ligand proportions (Cu: BTC 1.8: 1 and 1: 1), seeking the formation of highly organized metal-organic structures. Besides being synthesized in an aqueous environment, these MOFs were capable of capturing carbon dioxide, and contribute to the

development of sustainable materials. In summary, the results of the study and modification of the methods collaborated significantly to the improvement of MOF syntheses and their applications.

Keywords: Metal-organic frameworks (MOFs), Self-assembled monolayer (SAM), Silica functionalization, Morphology, Carbon dioxide, Adsorption and desorption cycles



## LIST OF FIGURES

Figure 1. Secondary building units (SBUs) commonly observed in metal-organic frameworks <sup>11</sup> (A) binuclear paddle-wheel; (B) trinuclear hourglass; (C) trinuclear prism; (D) tetranuclear cuboid; (E) tetranuclear octahedron .....	12
Figure 2. Linkers commonly used in the synthesis of MOFs <sup>11</sup> .....	12
Figure 3. Modular structure of MOFs using Cu <sub>3</sub> (BTC) <sub>2</sub> as an example <sup>21</sup> .....	14
Figure 4. Overview of synthesis methods (adapted) <sup>26</sup> .....	16
Figure 5. Obtaining of the first thin films of MOFs <sup>7</sup> (adapted).....	17
Figure 6. Schematic representation of the SAM structure constituted of a head group (-SH), tail (R) and functional terminal group (X) <sup>28</sup> .....	18
Figure 7. Growth of MOFs <sup>32</sup> .....	20
Figure 8. Configuration for the manufacture of fine films by the spraying method. Legend: (1) gas, (2) gas flow controller (3) three gas distributing valves (4) container with the A, B, C sprayed solutions (5) sample holder (6) dosing valves (7), spray chamber <sup>27,33</sup> .....	20
Figure 9. Schematic diagram of the growth of MOF films <sup>32-34</sup> .....	21
Figure 10. Schema of activated SBA-15 silica surface with OH-terminated groups .....	24
Figure 11. Schema of simple spray method employed for the fabrication of MOF thin films: (a) sample holder, (b,c) solutions containers, (d) gas supply, (e) gas flow controller, (f) dosing valves .....	28
Figure 12. Illustration of (a) activated SBA-15 silica. (b) activated SBA-15 silica with Cu-BTC deposition. (c) gold with MHDA-SAM. (d) gold with MHDA-SAM and Cu-BTC deposition.....	29
Figure 13. Out-of-plane data for Cu <sub>3</sub> (BTC) <sub>2</sub> (a) growth on OH- activated SBA-15 silica substrate and (b) growth on MHDA SAM on gold substrate.....	30
Figure 14. FTIR spectra of (a) Cu-BTC on gold substrate, (b) Cu-BTC on SBA-15 silica substrate and (c) SBA-15 silica .....	31
Figure 15. SEM images of (a) SBA-15 pastille, (b) SBA-15 + Cu-BTC by LBL spray method, (c) gold substrate + MHDA-SAM + Cu-BTC and TEM images of (d) gold + MHDA SAM + Cu-BTC (e) SBA-15 silica and (f) SBA-15 + Cu-BTC by LBL spray method .....	33

Figure 16. Illustration of the dispersion of nanoparticles by using high energy ultrasonic homogenizer to MOF preparation .....	38
Figure 17. Process of obtaining MOFs: (a) mixture of copper and BTC precursors, (b) separation of the two phases (MOF and solvent) characteristic of the formation of the MOF and (c) final MOF powder. ....	38
Figure 18. Powder X-Ray diffraction patterns simulated from the crystallographic data of $\text{Cu}_3(\text{BTC})_2$ (ref. <sup>71</sup> ), and samples synthesized by using high energy sonicator: 1 min and 5 min. ....	40
Figure 19. FTIR spectrum of $\text{H}_3\text{BTC}$ and $\text{Cu}_3(\text{BTC})_2$ sample synthesized by 1 min ultrasonic homogenizer .....	41
Figure 20. TG/DTG of $\text{Cu}_3(\text{BTC})_2$ sample synthesized with ultrasonic homogenizer .....	42
Figure 21. SEM images of Cu-BTC by one minute ultrasonic irradiation homogenizer under different pressures (a) autoclave, (b) ambient pressure; and TEM images of Cu-BTC by one minute ultrasonic irradiation homogenizer both (c) and (d) under autoclave. ....	43
Figure 22. Process of obtaining MOFs: (a) mixture of copper and BTC precursors, (b) separation of the two phases (MOF and solvent) characteristic of the formation of the MOF and (c) final MOF powder. ....	48
Figure 23. Powder X-Ray diffraction pattern simulated from the crystallographic data of $\text{Cu}_3(\text{BTC})_2$ <sup>78</sup> (down), and synthesized sample (top). ....	49
Figure 24. FTIR spectrum of $\text{H}_3\text{BTC}$ and $\text{Cu}_3(\text{BTC})_2$ sample synthesized .....	50
Figure 25. SEM and TEM images illustrate how the morphologies of Cu: BTC 1.8:1 and CuBTC-1:1 change with the molar ratio between Cu and BTC. SEM images of Cu-BTC 1.8:1 ratio (a) and (b); SEM (c) and TEM (d) images of Cu:BTC 1:1 ratio. ....	52
Figure 26. TG/DTG of Cu-BTC synthesized sample .....	53
Figure 27. $\text{CO}_2$ adsorption–desorption for 1.8:1 Cu:BTC sample at 30 °C adsorption and 100 °C desorption. ....	54
Figure 28. Cycle of $\text{CO}_2$ adsorption–desorption for 1.8:1 Cu:BTC sample at 30 °C adsorption and 100 °C desorption. ....	55

## LIST OF ABBREVIATIONS

Fourier transform infrared spectroscopy (FTIR)

Hong Kong University of Science and Technology (HKUST-1)

Metal nodes of copper connected with trimesic acid as ligands (Cu-BTC)

Metal-organic frameworks (MOF)

Scanning electron microscopy (SEM)

Self-assembled monolayer (SAM)

Thermogravimetric analysis (TG)

Thin film metal-organic framework (SURMOF)

Transmission electron microscopy (TEM)

X-ray diffraction (XRD)

## OUTLINE

CAPÍTULO 1. Introdução .....	1
CHAPTER 1. Introduction .....	2
1.1 Motivation .....	2
1.2 Objectives .....	5
1.3 Thesis structure and organization .....	7
CHAPTER 2. Literature review.....	9
2.1 Metal-organic frameworks (MOFs).....	9
2.1.1 Methods of obtaining MOFs .....	15
2.2 Thin film MOFs (SURMOFs) .....	17
2.2.1 Anchoring groups between support and SURMOF .....	19
2.2.1 Layer-by-layer deposition procedure by spray .....	19
2.3 MOF for CO <sub>2</sub> Adsorption .....	21
CHAPTER 3. Room temperature and ambient pressure deposition of Cu-BTC MOF on SBA-15 functionalized silica supports by simple spray layer-by-layer method .....	23
3.1 Introduction .....	23
3.2 Experimental .....	26
3.2.1 Materials.....	26
3.2.2 Substrate Preparation .....	26
3.2.3 Preparation of silica (SBA-15) substrates.....	26
3.2.4 Preparation of the metal-organic frameworks.....	27
3.2.5 Characterization .....	28
3.3 Results and Discussion .....	29
3.3.1 XRD.....	29
3.3.2 FTIR .....	30

3.3.3 SEM and TEM.....	32
3.4 Conclusions.....	34
CHAPTER 4. Production of rod-like morphology of Cu <sub>3</sub> (BTC) <sub>2</sub> metal-organic frameworks using one minute sonication .....	35
4.1. Introduction .....	35
4.2. Experimental .....	36
4.2.1 CuBTC preparation .....	36
4.2.2 Ultrasonic radiation interference experiments.....	36
4.2.3 Techniques used for characterization .....	36
4.3 Results and discussion.....	37
4.3.1 XRD.....	39
4.3.2 FTIR .....	40
4.3.3 Thermogravimetric analysis TG/Degradation .....	41
4.3.4 SEM and TEM.....	42
4.4 Conclusions.....	44
CHAPTER 5. Syntheses of environmentally-friendly Cu-BTC metal-organic frameworks with unusual morphology and potential to CO <sub>2</sub> capture .....	45
5.1. Introduction .....	45
5.2. Experimental .....	46
5.2.1 Cu-BTC H <sub>2</sub> O based preparation.....	46
5.2.2 Techniques used for characterization .....	47
5.3 Results and discussion.....	48
5.3.1 XRD.....	49
5.3.2 FTIR .....	50
5.3.3 SEM and TEM.....	51
5.3.4 Thermogravimetric analysis TG/Degradation .....	52



5.3.5 CO <sub>2</sub> uptake evaluation .....	53
5.4 Conclusions.....	55
CAPÍTULO 6. Considerações finais .....	57
CHAPTER 6. Final Considerations .....	58
REFERENCES.....	60

## **CAPÍTULO 1. Introdução**

Um dos maiores causadores do aquecimento global é a emissão de enorme quantidade de dióxido de carbono ( $\text{CO}_2$ ) para o meio ambiente. O rápido aumento da população tem proporcionado um crescimento explosivo no consumo de energia, sendo mais de 85 por cento supridas por combustíveis fósseis. A emissão desenfreada de poluentes provenientes dessa queima aumenta a emissão de dióxido de carbono e contribui para problemas globais, como a liberação de gases tóxicos e gases estufa. Nesse sentido, esforços consideráveis foram feitos para desenvolver tecnologias para captura de  $\text{CO}_2$ , incluindo absorção, adsorção, criogenia, membranas funcionais e zeólitas. No entanto, essas tecnologias apresentam algumas desvantagens, como, perda de solvente, corrosão de equipamentos e alto custo de regeneração. Nesse contexto, a combinação das propriedades adquiridas pela síntese de estruturas metalorgânicas (MOFs), objeto desse trabalho, tais como cristalinidade, porosidade e interações ligante-metal, aliadas às novas aplicações provenientes da variação dos parâmetros de síntese surgem como uma alternativa interessante para alcançar propriedades em escala ainda menores abrindo oportunidade, inclusive, para a utilização de adsorventes sintetizados a partir desses materiais <sup>1,2</sup>.

Esta pesquisa estudo buscou responder questões relativas à possibilidade de deposição de MOF em substratos cerâmicos, consolidar a tecnologia de produção de MOFs particulados na UFMG, substituir solventes orgânicos para fabricar MOFs mais compatíveis com o meio ambiente e avaliar suas possíveis aplicações na captura e seleção de gases. Nesse contexto, uma melhor compreensão da síntese e dos mecanismos de obtenção do Cu-BTC MOF (metal: cobre e ligante: ácido trimésico), variando condições de temperatura e pressão, e o estudo do seu potencial para interagir com materiais cerâmicos, representa uma contribuição relevante para os materiais porosos, tendo em vista a importância ambiental e tecnológica destes materiais.

## CHAPTER 1. Introduction

### 1.1 Motivation

One of the greatest causes of global warming is the emission of huge amounts of carbon dioxide (CO<sub>2</sub>) into the environment. Rapid population growth has led to explosive growth in energy consumption, with more than 85 percent supplied by fossil fuels. The unbridled emission of pollutants from this burning increases CO<sub>2</sub> emissions and contributes to global problems such as the release of toxic gases and greenhouse gases. Considerable efforts have therefore been made to develop technologies for CO<sub>2</sub> capture, including absorption, adsorption, cryogenics, functional membranes, zeolites, metal oxides and so on. However, these technologies have some inherent disadvantages, including low efficiency, solvent loss, equipment corrosion, high cost for regeneration.<sup>1,2</sup>

In this context, a study was conducted on the new class of porous materials with great potential to overcome these disadvantages: the metal-organic frameworks (MOFs).

MOFs are a new class of materials with well-defined properties. They are crystalline, highly porous and exhibit strong ligand-metal interactions. Its physical and chemical properties, including pore size and structure, acidity, and magnetic and optical characteristics may be adapted by selecting suitable binders and metal precursors or by post-synthesis treatments. In addition, MOFs may exhibit isolated polynuclear sites, specific interaction site-substrate and adjustable hydrophobicity<sup>3</sup>.

MOFs have received intense interest over the last decade because of their wide application. A recent estimate indicates more than 20,000 coordination network structures, which may be classified as MOFs, were listed in the Cambridge Structural Database (CSD), in 2014, and more than 70000 MOF combinations,

in 2017. They present many potential advantages over traditional nanoporous materials for various chemical technologies, such as catalysis, gas separation and adsorption, sensors and biomedical devices <sup>2,4</sup>.

MOFs are crystalline materials with structures based on classical coordination bonds between metal cations (e.g.,  $\text{Cu}^{2+}$ ,  $\text{Zn}^{2+}$ ) and electron donors such as carboxylates or amines. The self-assembly of these components, usually in solution, creates rigid pores that do not collapse upon removal of the solvent or other "guest" molecules that occupy the pores after synthesis. The presence of both inorganic and organic components allows both pore size and chemical environment to be adapted to achieve specific properties. This differentiates MOFs from zeolites, which are also crystalline and microporous, but are totally inorganic and therefore lack synthetic flexibility. The topology of MOFs is closely related to the coordination environment favored by the metal ion and the geometry of the organic "linker" groups, which together form the so-called secondary building units that establish the symmetry of the network. These characteristics further distinguish MOFs from other classes of porous materials, such as aerogels, which are amorphous, and ordered or partially ordered materials created from block copolymers <sup>5</sup>.

Various techniques, such as direct synthesis, surface functionalization methods, and others have been reported for the fabrication of MOF. One of the approaches consists in the use of interfaces to initiate and control the growth of MOFs in terms of orientation and crystallinity. They are called surface-anchored metalorganic frameworks (SURMOFs) <sup>6-8</sup>.

MOFs are already studied by many institutes around the world. In Germany, the recognized Institute of Functional Interfaces of the Karlsruhe University (IFG/KIT) is a reference on SURMOF research. During undergraduation, the

author completed a sandwich period in Germany, at IFG/KIT, where she could start a project in SURMOFs. As a result of this period, she brought this technology to the Department of Metallurgical Engineering of UFMG, where MOF and SURMOF technology have been consolidated through this partnership, being the pioneer in SURMOF at UFMG.

Besides of SURMOFs, another approach is to produce particulate MOFs. They are synthesis by hydrothermal or solvothermal process. The MOF material forms small crystals in a hot solution (120°C – 150°C) of the metal precursors and the ligands. The individual powder particles are formed by self-assembly in the solution, creating complex, three-dimensional, highly porous network structures with perfect translational symmetry. Some MOF types do not need heating, e.g., the MOF HKUST-1 may be produced by simply mixing room temperature solutions of  $\text{Cu}^{2+}$  ions (Cooper-acetate) and 1,3,5-benzyl tricarboxylic acid ( $\text{H}_3\text{BTC}$ ). In HKUST-1 MOF type, the carboxylate groups ( $-\text{COO}-$ ) of the BTC ligand are coupled by metal clusters. With the aforementioned properties, MOFs have been applied to the various components of the  $\text{CO}_2$  cycle.<sup>7,9</sup>

This research was conducted on the Laboratory of Ceramics Materials (LMC/UFMG) that has expertise in nanotechnology, adsorbent materials, structurology, ceramic membranes sol-gel technology and composites, among others. The LMC main focus is on environmental solutions such as gas selective/capture porous materials. In this way, the present MOF research was directed to the study of porous materials with potential for application in environmental issues and the possibility of association of MOF and ceramic materials.

This study seeks to answer questions such as the possibilities of deposition of MOF on ceramic substrates, consolidate the bulk MOF technology,



manufacturing of MOF/silica blends and their potential applications in gas uptake and selection. In this context, a better understanding of Copper-BTC MOF synthesis and mechanisms under low-temperature and low-pressure conditions, and its potential to interact with ceramic materials represents a relevant contribution to porous materials, in view of the environmental and technological importance of this MOF.

## **1.2 Objectives**

The aim of this thesis is to continue the developed research by the doctorate during the sandwich undergraduation program held at the Institute of Functional Interfaces (IFG) at the University of Karlsruhe (KIT), where she learned how to synthesize the metal-organic framework surfaces (SUR-MOFs) and the first steps in its characterization by Electronic Transmission Microscopy (MET). After this period the author consolidated this new technology in Brazil through the works that have been done at UFMG. The partnership with the Laboratory of Ceramic Materials (LMC/UFMG) has proved very promising, as the porous materials produced at IFG/KIT have properties that fit with the main objective of the LMC/UFMG: development of porous materials for gas adsorption. In addition, the research group on surface functionalization at the University of Karlsruhe is interested in continuing this research to obtain the same response regarding the gas capture. Thus, this project contributes significantly to the consolidation and continuation of scientific cooperation between Brazil and Germany.

This research work concentrates in the synthesis of both (A) Copper-BTC SURMOF using gold-coated and silica supports via liquid-phase epitaxy (LPE) layer by layer (LBL) synthesis with potential for application in gas separation and (B) MOF-bulk synthesis using dimethylformamide (DMF) and water via sonochemical and solvothermal methods with potential for gas uptake application.

### 1.2.1. Specific objectives

The first part of this work consisted of developing synthesized and characterized a Cu-BTC MOF on mesoporous SBA-15 silica substrate by using the layer-by-layer spray method. The following objectives were respected:

- Obtain the SBA-15 pastilles by using “evacuable pellet press dies” and activated with the necessary OH-terminated groups.
- Elaborate a granulation process for nanomaterials. Anchor the MOF on the silica surface.
- Design a spray layer-by-layer equipment, capable of working under room temperature and ambient pressure to produce MOF films.
- Evaluate the synthesis of SURMOF on mesoporous materials by the spray method designed.

The second part involved the ultrasonic homogenization technique to  $\text{Cu}_3(\text{BTC})_2$  formation. The listed aims below were respected:

- Evaluate the necessary time and power under ultrasonic irradiation to prepare the material.
- Design a rod-like MOF under room pressure.
- Optimize the process of the MOF synthesis by using sonicator.

The third part is based on obtaining the water-based MOF Cu-BTC synthesized with excess metal and evaluate the morphology and  $\text{CO}_2$  capture capacity. The following objectives were respected:

- Evaluate the interference in the morphology by the ratio ligand/metal.
- Design a crystalline MOF with well-defined structure.

- Analyze the effect of the MOF concentration in adsorption performance, and repeatability during cycles of adsorption/desorption.

### 1.3 Thesis structure and organization

This thesis is structured in 6 chapters. **Chapter 1** provides an introduction to the theme of this investigation and a summary of the Institute of Functional Interfaces (IFG/KIT - Germany) and Laboratório de Materiais Cerâmicos (LMC/UFMG - Brazil) research partnership.

**Chapter 2** offers a detailed and critical literature review on metal-organic frameworks (MOF); MOF in situ crystallization method; thin film MOFs (SURMOFs); self-assembled monolayers (SAM); spray method deposition, and analytical techniques used in the present investigation.

**Chapter 3** presents an investigation of Copper-based thin film metal-organic framework (SURMOF), HKUST-1, deposition on gold and SBA-15 silica substrates. They were characterized by using X-Ray Diffraction, Infrared Spectroscopy and Scanning Electron Microscopy with potential to gas separation membranes.

In **Chapter 4**, a bulk Copper-based metal-organic framework was obtained under different conditions, such as, temperature sources (autoclave and furnace); and variation of time and power of ultrasonic radiation. It was analyzed by X-ray diffraction, Infrared spectroscopy, Thermogravimetry degradation and SEM and TEM morphology analysis. The best condition was used to develop a new adsorbent MOF material with rod-like shape.

In **Chapter 5**, a water-based environmentally friendly bulk Copper-MOF was obtained. It was analyzed by X-ray diffraction, Infrared spectroscopy, Thermogravimetry degradation and SEM and TEM images. Changing the Cu:BTC ratio, unusual morphology was obtained. It was tested such as carbon dioxide adsorption using thermogravimetric machine.

Finally, **Chapter 6** contains the final considerations of the study, the conclusions and suggestions to future works.

## CHAPTER 2. Literature review

### 2.1 Metal-organic frameworks (MOFs)

Coordination polymers have been known for several years. In 1954, Wells published the concept of inorganic crystalline structures, demonstrating the participation of metal ions, acting as nodes, and connecting with each other with spacers in a structure similar to the multidentified organic molecules of the coordinating polymers. This formed network, as well as its topology, depends on the geometry and the coordination environment of the nodes, the spacer being only a linear connection between adjacent nodes <sup>10,11</sup>.

In 1959, it was published an interesting study on coordinating crystalline polymers, where was described the structure of copper compounds associated with nitrate anions. However, the porosity received little attention. In mid-1989, researchers returned to writing about polymeric networks, now made up of three-dimensional segments with connecting pillar units showing these materials so rich with information. Subsequent works highlight the potential use of these materials in diverse applications. The term “metal-organic framework” appeared in the literature of journals only in 1995 with Yaghi's group <sup>11–13</sup>.

The study of coordination polymers gained great prominence with the development of materials with permanent porosity and thermally and chemically stable. The first successful work that can be considered as the beginning of the MOF study was published by Li et al. (1999), where the synthesis of a coordination polymer of very high porosity and stability was carried out. Named as MOF-5, the researchers synthesized a 3-D MOF with groups of  $Zn_4O$  and terephthalic acid as a ligand,  $[Zn_4O(BDC)_3]$ , and formed a cubic structure and a three-dimensional porous system <sup>11,13</sup>.



This fascinating class of crystalline hybrid materials is formed by associations of metallic centers or agglomerates and organic binders and offers unique chemical versatility, large and permanent internal porosity. As such, MOFs constitute their own family of porous materials that overcome the limitations of already known porous materials (zeolites, mesoporous silica, activated carbon)<sup>3,14</sup>.

At the beginning, most of the efforts were directed towards the synthesis of structures with new topologies and with the largest possible surface areas. The aim was to find materials with exceptionally high gas storage capacities, especially hydrogen. Recently, structures were synthesized with better control of properties through external parameters (for example, a host molecule or physical stimulus)<sup>3,14</sup>.

Metal-organic frameworks encouraged researchers due to their versatility and extended chemical functionalization in relation to zeolites. During the past few years, some of these goals have started to be realized around the concepts of isorecticular structures, synthesis, functionalization, coating, solid solution, varied structures (copolymer) and hybrid crystal approaches. The novelty is the adjustment of organic ligands and the possibility of incorporating reactive groups inside MOFs<sup>11</sup>.

Efforts to improve the synthesis of these materials and the selections for industrial and processing applications are increasingly present in several sectors. In particular, the use of MOFs as films is one of them, which is important for many applications, such as chemical sensors and membranes. It is worth mentioning that almost 50% of the works on this theme (MOFs as coverings) were published after 2011, which corroborates the currentness of the theme<sup>3,11,14</sup>.

The new class of metal-organic materials (MOFs) has well-defined properties such as crystallinity, porosity and strong binder-metal interactions. Its properties can be adapted by selecting suitable binders and metal precursors or through post-synthesis treatments. In addition, MOFs may have isolated polynuclear sites, specific active site-substrate interaction and a cavity environment with adjustable hydrophobicity <sup>11</sup>.

The MOF synthesis occurs by the addition of a metal solution and another solution containing organic ligand component. After this contact, the process of self-assembly occurs, in which the metals or clusters form the "knots" and the organic molecules form the "paddles", which, as ligands, transfer the electrons in the coordination bond with the metal center <sup>13</sup>.

Inside the structure, it's possible to verify the presence of other molecules as CO<sub>2</sub>, H<sub>2</sub>O, Cl<sub>2</sub>, CN<sup>-</sup>, etc. The molecules geometry can be found in many forms, for example the secondary building units (SBUs) usually composed of only one metal atom. There are also the single-metal-ion-based molecular building block (MBB). It can be obtained in situ through the use of metal ions with multifunctional linkers <sup>15-18</sup>.

There is also the formation of clustering of metallic atoms (cluster) forming several geometries, as shown in Figure 1: (A) binuclear paddle-wheel; (B) trinuclear hourglass; (C) trinuclear prism; (D) tetranuclear cuboid; (E) tetranuclear octahedron. One of the most common. In this case, two metal atoms are linked to four carboxylic groups, with the two oxygen atoms of the same carboxylic group making a kind of bridge with the two metal atoms <sup>11,18</sup>.

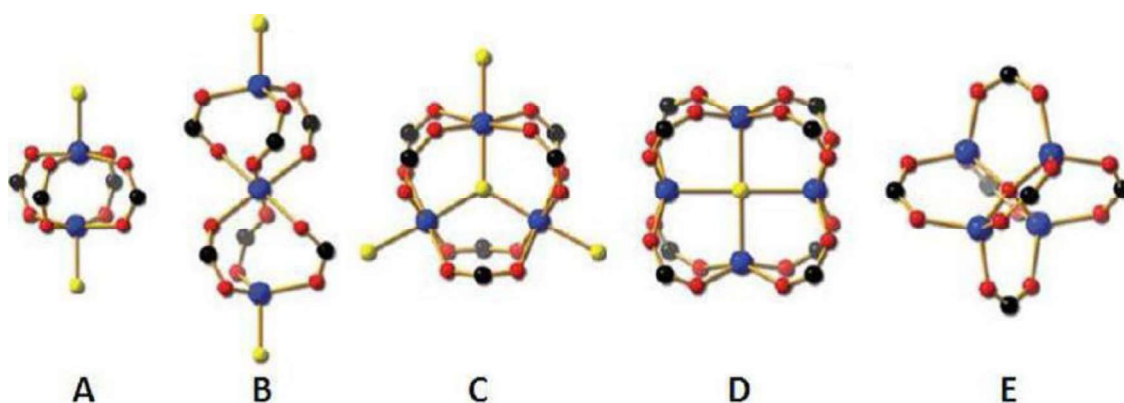


**Figure 1. Secondary building units (SBUs) commonly observed in metal-organic frameworks <sup>11</sup> (A) binuclear paddle-wheel; (B) trinuclear hourglass; (C) trinuclear prism; (D) tetranuclear cuboid; (E) tetranuclear octahedron**

There are several compounds that can be used as organic linkers. Polycarboxylated aromatic molecules, bipyridines and poly-heteroaryl cyclic molecules (imidazole, triazole, tetrazole, pyrimidine, pyrazines, etc.) are very common. Figure 2 shows the most commonly used binders.

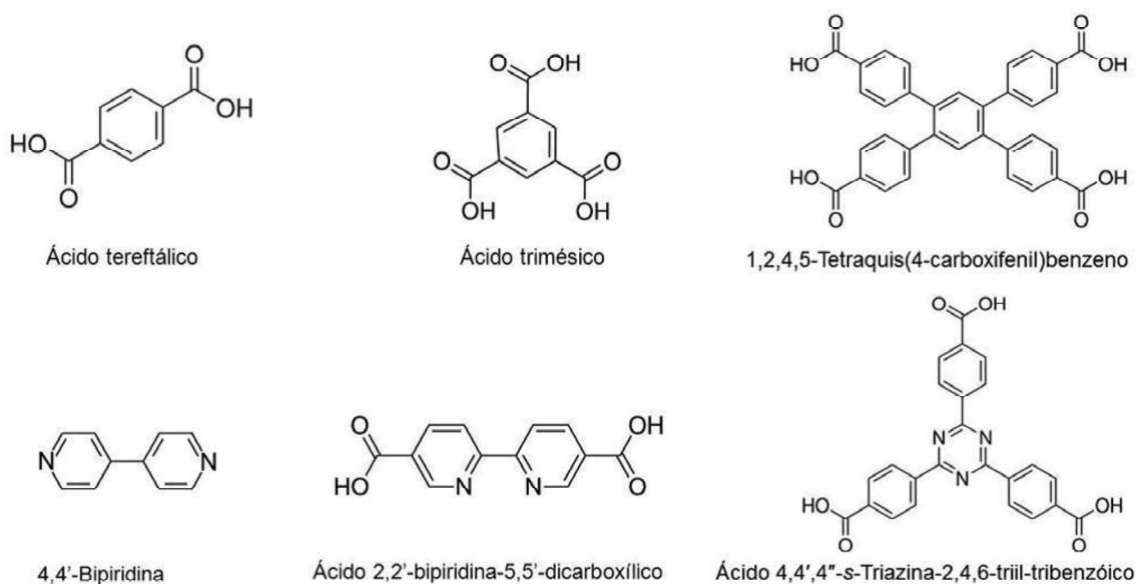


**Figure 2. Linkers commonly used in the synthesis of MOFs <sup>11</sup>**

What defines the choice of the linker is the position of the coordination groups on the ligand molecules in order to design the final structure of the MOF. In the work presented by Paz et al. (2012),<sup>19</sup> it is possible to perceive the relationship between the nature and the structure of organic linkers. They systematized in a table a compact library of synthetic paths to various families of compounds to encourage and assist researchers to design new MOFs. It shows how this choice is based on the wish properties to obtain in products.

The collection of MOFs includes the so-called HKUST-1, Figure 3, named of the institution that gave rise to it (Hong Kong University of Science and Technology), formed by copper as metal and 1,3,5-benzenetricarboxylic acid (BTC) as a ligand  $[\text{Cu}_3(\text{BTC})_2]$ , the so-called MOF-5, where zinc is the metal and 1,4-dicarboxylic acid (BDC) participates as a ligand  $[\text{Zn}_4\text{O}(\text{BDC})]$ . In addition to several others such as zeolitic imidazolate frameworks (ZIF) and nanofilms on solid surfaces (NAFs) and their associations<sup>15,20</sup>.

Although porous MOFs have developed quite recently, they already have a number of advantages: their synthesis is relatively simple and flexible. This is possible due to the choice of metal and organic binder and the way they are connected. Zeolites and similar compounds (aluminophosphates, silicoaluminophosphates) do not have this flexibility, since the secondary construction unit (SBU) are tetrahedra of silica and alumina, with rigid and well-defined bonds between Si/Al atoms with oxygen, not being so easy to change chemical composition and structure, making the main applications related to small host molecules within the structure<sup>11</sup>.

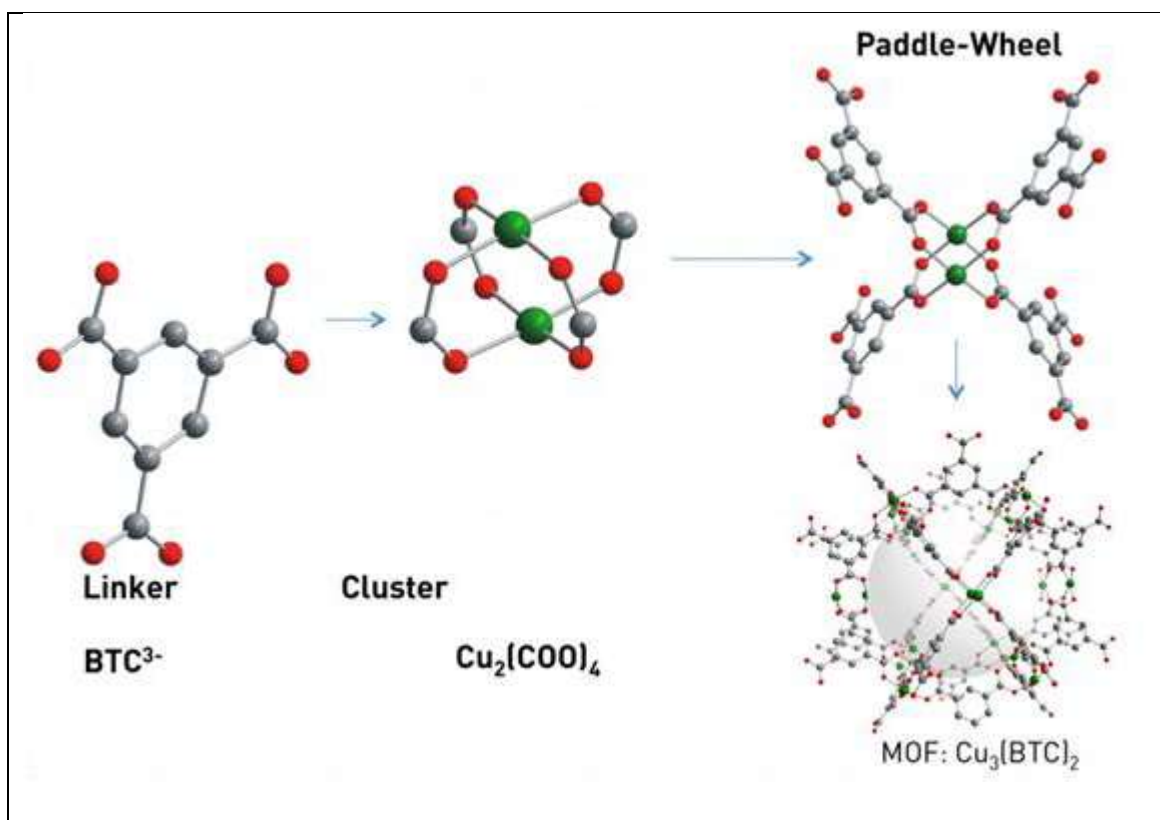


**Figure 3. Modular structure of MOFs using  $\text{Cu}_3(\text{BTC})_2$  as an example** <sup>21</sup>

In relation to the porous properties, due to the varied possibility of control, MOFs can act as molecular membranes, selecting the molecules that can diffuse in the pores. In this way, MOFs fill a gap between non-porous surface organometallic catalysts, microporous zeolites and mesoporous silicates <sup>11,22</sup>.

The presence of strong metal-binder interaction can (and should) confer permanent porosity to the material, even after the removal of solvent molecules, without collapse of the structure. The surface area, the ease of adjusting the pore size and other properties made one of its first real applications to be in the area of gas separation and storage <sup>11,22</sup>.

In the literature we find several interesting applications, among them the purification, separation and storage of gases, the separation of CO<sub>2</sub> from gaseous emissions being one of the most promising applications <sup>11,23,24</sup>. MOFs are also being synthesized through reactions that favor the confinement effect, with dispersion of nanomaterials and carrying active ingredients of drugs with controlled release (drug delivery) <sup>16,25</sup>.

Other interesting works address the use of MOFs applied as chemical sensors, based on magnetic and optical properties. Some MOFs have their magnetic properties altered when they store or release visiting molecules due to reversible structural transformations, either due to the change in amorphous to crystalline structure, or a transformation of crystalline phases. In this way, they can be used as molecular recognition sensors <sup>11</sup>.

### **2.1.1 Methods of obtaining MOFs**

Stock et al show on its study many forms of obtaining MOFs. The Figure 4 illustrates examples of some methods. The definition of conventional or solvothermal procedure is not consolidated in the literature; basically precursor reagents are placed in the autoclave and submitted to temperatures above the solvent boiling point. The electrochemistry process use copper electrodes or other metals as metal source. The microwave is also an alternative energy source. The sonochemistry method consists on using ultrasound energy on liquids to promote alternating cyclical areas of compression (high pressure) and rarefaction (low pressure) <sup>26</sup>.

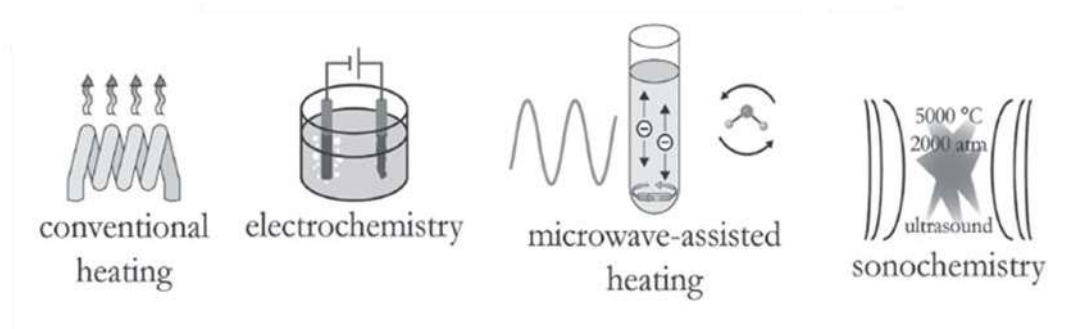
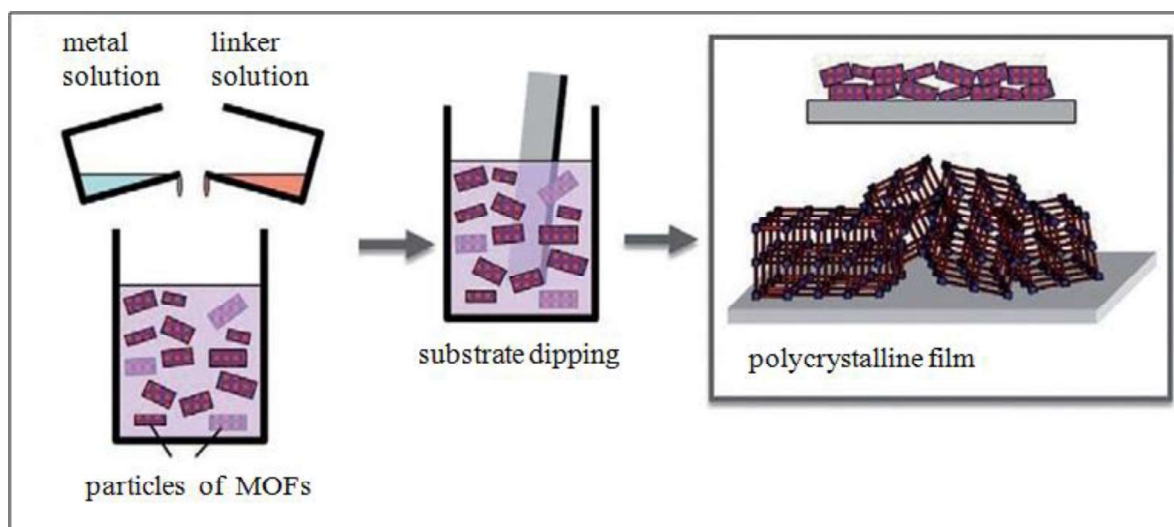


Figure 4. Overview of synthesis methods (adapted) <sup>26</sup>

According to Gliemann and Wöll (2012), the synthesis of particulate MOF is usually carried out in a hydrothermal or solvothermal process: a solution containing the metal precursors and the binders is heated and the MOF is formed as small crystals. Some types of MOF do not even need heating, for example, HKUST-1 MOF can be produced simply by mixing the solutions of  $\text{Cu}^{2+}$  ions (Cu acetate) and 1,3,5-benzyl tricarboxylic acid ( $\text{H}_3\text{BTC}$ ) at room temperature. Although the MOF obtained in powder form is suitable for many applications (such as gas storage on an industrial scale), other applications require solid substrates coated with MOFs so they are immobilized on the surface.

The simplest method is to immerse a substrate in a suspension of MOF particles previously precipitated from a mixture of a solution containing metal ions and the ligand. Figure 5 illustrates the coating of a substrate with particulate MOF, which was precipitated before the coating.



**Figure 5. Obtaining of the first thin films of MOFs <sup>7</sup> (adapted).**

This method produces a very heterogeneous coating and does not uniformly cover the substrate. The films have different orientation and sizes, which may not be directly connected to the substrate.

## 2.2 Thin film MOFs (SURMOFs)

The SURMOF obtaining process is based on the formation of a self-assembled monolayer (SAM) anchored to the three-dimensional structure composed a metal (in this case copper or zinc) atoms connected to each other by acid products via layer-by-layer methodology <sup>7,27</sup>.

The self-assembled monolayers of organic molecules are spontaneously molecular formed on adsorption surfaces and organized into ordered domains. The molecules constituting the monolayer may interact strongly with the substrate or have a functional group which has a strong affinity to the substrate and anchors the molecule. SAM is constituted of a head group (-SH), tail (R) and functional terminal group (X), as shown in Figure 6 <sup>28</sup>.



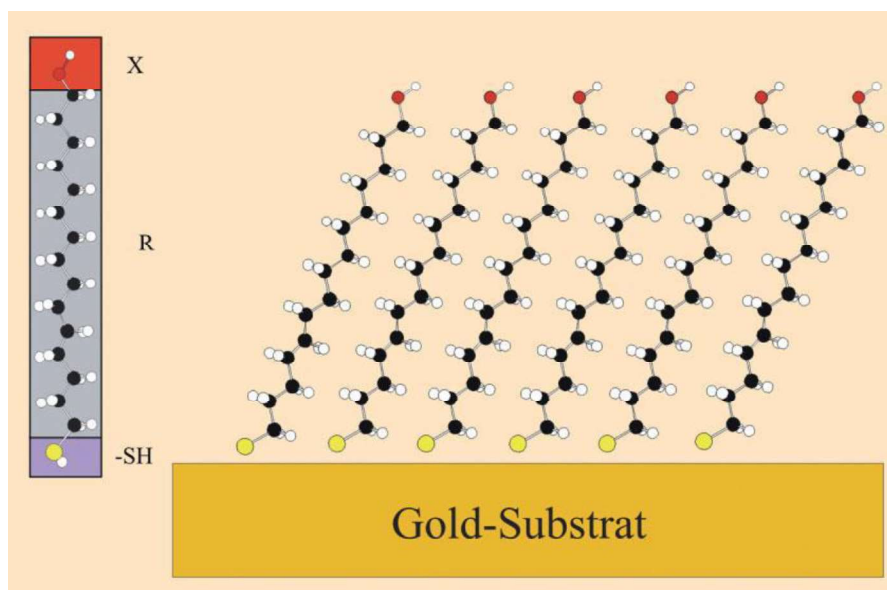


**Figure 6. Schematic representation of the SAM structure constituted of a head group (-SH), tail (R) and functional terminal group (X) <sup>28</sup>**

The SAMs production, unlike most surface technologies, is simple. The formation of highly ordered films is fast and exhibits low cost processes with few defects. In addition, self-assembled monolayers may be formed on a rough, uneven surface, internal surfaces and difficult to access for most methods <sup>28</sup>.

Anchored to the SAMs surfaces, Metal-Organic Frameworks (MOFs) with a new class of materials with well-defined properties are going to grow. They are crystalline, highly porous and exhibit strong ligand-metal interactions. Its physical and chemical properties, including pore size and structure, acidity, and magnetic and optical characteristics may be adapted by selecting suitable binders and metal precursors or by post-synthesis treatments. In addition, MOFs may exhibit isolated polynuclear sites, specific interaction site-substrate and adjustable hydrophobicity. The functionalization of surfaces due the building of MOFs on their structure opens opportunity of little explored applications <sup>3,14</sup>

### **2.2.1 Anchoring groups between support and SURMOF**

The growth of SURMOF is not limited to gold substrates, but can occur in materials where the surface of the substrate can be functionalized with the respective terminals of the ligand molecules. According to Jinxuan et al. (2010)<sup>29</sup>, SAMs can be prepared on various substrates, metallic or semiconductors, for example, Au, Ag, Cu, Pt and Pd for metallic substrates, SiO<sub>2</sub>, Al<sub>2</sub>O<sub>3</sub>, TiO<sub>2</sub>, ZnO for semiconductor surface, in addition to substrates modified with SAM based on silane. The most used substrate is gold because it is an inert metal and is not oxidized at room temperature in the air; and can be used for many other surface analytical techniques.

The mesoporous Santa Barbara Amorphous type material (SBA-15) is another interesting substrate due to properties such as uniform pore size, hexagonal and cylindrical channels and large surface area, when compared to the silica gel typical materials. In addition, the SBA-15 silica presents OH-terminated groups on the silica surface, which allows the incorporation of new materials in the silica structure<sup>30,31</sup>.

### **2.2.1 Layer-by-layer deposition procedure by spray**

The preparation of the SURMOFs can be performed on the formed monolayer similar to that presented by Shekhah et al.<sup>32</sup> Figure 7 illustrates the step-by-step growth of MOFs over SAM through repetitive cycles of the precursor metal solution and subsequently of the organic linker solution.

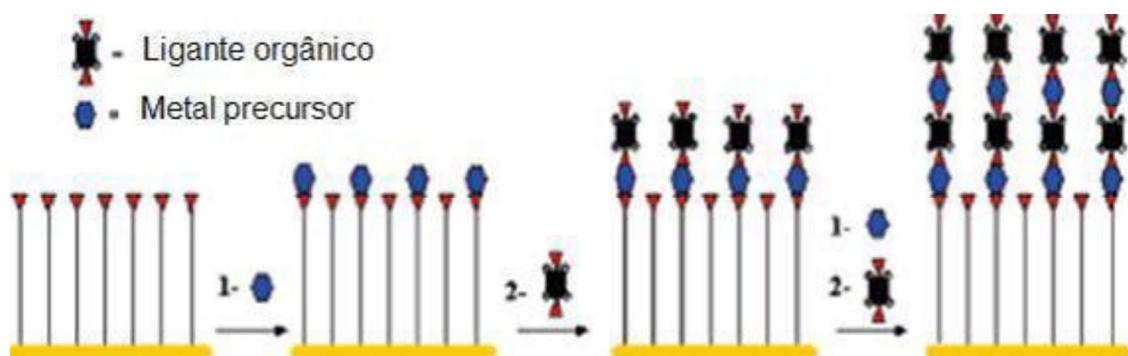


Figure 7. Growth of MOFs <sup>32</sup>.

The layers of the metal and organic linker to form the metal-organic frameworks are going to be deposited by the layer-by-layer method. Figure 8 shows the assembly and organization scheme of the reagents as well as the position of the sample.

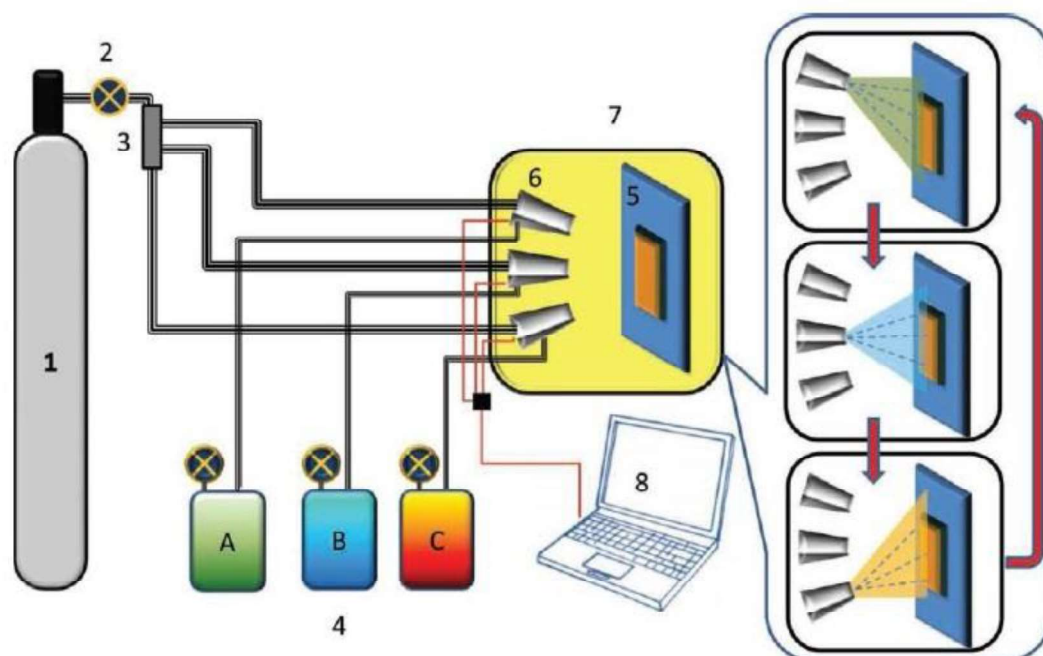


Figure 8. Configuration for the manufacture of fine films by the spraying method. Legend: (1) gas, (2) gas flow controller (3) three gas distributing valves (4) container with the A, B, C sprayed solutions (5) sample holder (6) dosing valves (7), spray chamber <sup>27,33</sup>

Each sample can be sprinkled in different cycles. From one cycle to another, washes are performed to allow the desired growth of the structure according to the scheme shown in Figure 9. At the end of the cycles the samples can be directed to the characterization analyzes.

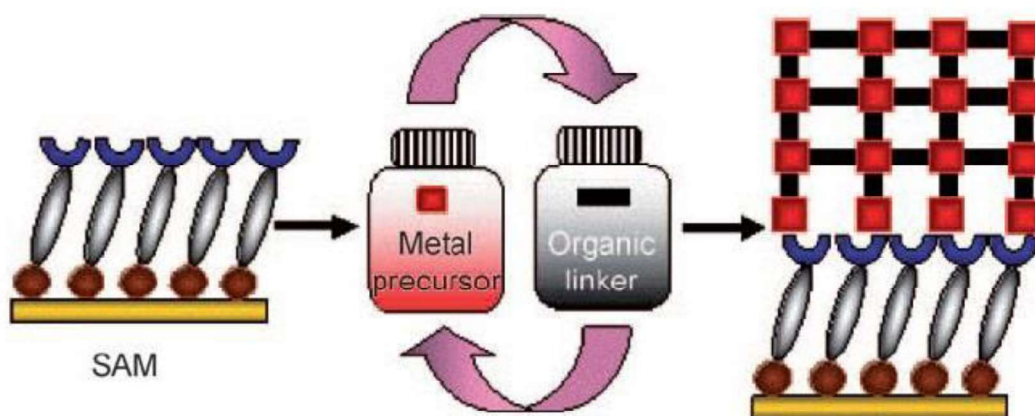


Figure 9. Schematic diagram of the growth of MOF films <sup>32-34</sup>

### 2.3 MOF for CO<sub>2</sub> Adsorption

Metal–organic framework compounds offer as mentioned before, enormous opportunities of different applications, such as catalysis, drug delivery and sensors <sup>35-38</sup>. It may also be used as adsorbent materials and gas separation membranes <sup>9,22,39</sup>. In this sense, MOFs have different CO<sub>2</sub> adsorption mechanisms depending on their structure properties <sup>40,41</sup>.

The CO<sub>2</sub> adsorption phenomena for MOF materials depends on many factors, such as capacity, enthalpy of adsorption and selectivity for CO<sub>2</sub> <sup>42</sup>. The gravimetric adsorption capacity refers to the amount of adsorbed CO<sub>2</sub> within the mass of the material and determines the quantity of the MOF needed to form the adsorbent bed. The volumetric capacity refers to the CO<sub>2</sub> density that can be stored in the material and significantly influences the volume of the adsorbent bed. The high internal surface areas of the metal-organic structures

offer an opportunity for great CO<sub>2</sub> adsorption capacities, due to the efficient packaging and the close approach of the guest molecules on the pore surface<sup>42</sup>.

The enthalpy of adsorption of CO<sub>2</sub> has influence over the performance of materials to CO<sub>2</sub> capture applications. It determines the affinity of the pore surface toward CO<sub>2</sub>. It has a role in determining the adsorptive selectivity and the energy required to release the CO<sub>2</sub> molecules during regeneration. If the material binds CO<sub>2</sub> too strongly, for example, it would increase the regeneration cost due to the large amount of energy required to break the framework-CO<sub>2</sub> interactions. On the other hand, if the enthalpy of adsorption is too low, the material would be more readily regenerated but, the purity of the captured CO<sub>2</sub> would be lowered due to the decreased adsorption selectivity, and the volume of the adsorbent beds would also be increased due to the lower density of CO<sub>2</sub> adsorption<sup>42,43</sup>.

Finally, another relevant factor for adsorption is its selectivity for CO<sub>2</sub>. Essential for gas mixture applications, selectivity may originate from two main mechanisms. In sizebased selectivity (kinetic separation), a metal-organic framework with small pore size may permit molecules only up to a certain kinetic diameter to diffuse into the pores, allowing the molecules to be separated based on size<sup>42</sup>. In adsorptive selectivity (thermodynamic separation), there is a difference in affinity of the various components of the gas mixture to be adsorbed on the pore surface of the MOF. This selectivity may base upon a physisorptive adsorption mechanism, the separation relies on the gas molecules having different physical properties, such as the polarizability or the quadrupole moment, resulting in a higher enthalpy of adsorption of certain molecules over others. The other adsorptive selectivity can arise due to chemical interactions between certain components of the gas mixture and surface functionalities of the metal-organic framework (chemisorption)<sup>42,44</sup>.

## **CHAPTER 3. Room temperature and ambient pressure deposition of Cu-BTC MOF on SBA-15 functionalized silica supports by simple spray layer-by-layer method**

### **Abstract**

Metal-organic frameworks (MOFs) have received intense interest over the past decade due to its wide application such as catalysis, membrane-based gas separation, gas adsorption, sensing, and biomedical devices. Growth of MOFs on different solid surfaces allows improving their mechanical properties. Silica is a potential candidate. Due to the difficulty of rising Cu-BTC MOF on silica substrate our group was motivated to achieve a successful coating. This work outlines the functionalization of the gold surface through the MHDA self-assembled monolayer (SAM) and the construction of a MOF film (SURMOF) of Cu-BTC upward. The same MOF was also grown onto a modified mesoporous SBA-15 silica substrate. The first obtained silica particles were previously conformed and activated to receive the MOF. The layer-by-layer method was used to deposit MOF onto the substrates. The deposited MOFs films were characterized by X-ray diffraction (XRD), Fourier transform infrared spectroscopy (FTIR), scanning electron microscopy (SEM) and transmission electron microscopy (TEM) showed SBA-15 as a potential MOF support.

Keywords: silica functionalization, metal-organic framework, self-assembled monolayer

### **3.1 Introduction**

Metal-organic frameworks (MOFs) are crystalline and nanoporous materials comprised of small metal-containing clusters connected three-dimensionally by organic ligands <sup>45</sup>. They present a high apparent surface area, selective uptake

of small molecules and a large pore size. Due to its hybrid architecture, the MOFs represent a major advance in development of ordered porous media, which have attracted significant interest in the last ten years <sup>10,46</sup>.

The association of mesoporous silica materials with thin films has promoted their use into many interesting applications such as gas separation membranes, chemical sensors, optical and electrical devices, catalysis, among others <sup>30</sup>. Furthermore, inorganic porous membranes often show high performance to gas separation due to their defined pores in the scale of the size of molecules to be separated. In this way, membranes based on MOFs materials may offer potential to achieve similar applications <sup>47</sup>.

The MOF  $\text{Cu}_3(\text{BTC})_2$ , a coordination compound formed by copper and trimesic acid, also known as Cu-BTC and HKUST-1, is one of the widely studied MOFs <sup>21,48</sup> with notable potential for thin films <sup>49</sup>. In this sense, recent studies have been done to use mesoporous silica as support materials <sup>8,50</sup>. The mesoporous Santa Barbara Amorphous type material (SBA-15) presents particular features, such as uniform pore size, hexagonal and cylindrical channels and large surface area, when compared to the silica gel typical materials. In addition, the SBA-15 silica has the advantage of no need to pre-treat the surface before modification due to the silanol groups on the silica surface, as shown in Figure 10. The presence of these groups allows the incorporation of new materials in the silica structure <sup>30,31</sup>.

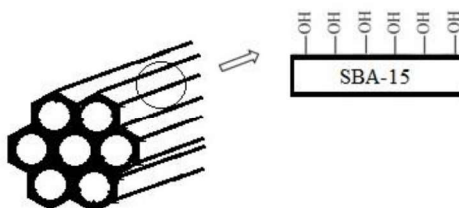


Figure 10. Schema of activated SBA-15 silica surface with OH-terminated groups

For many advanced applications in nanotechnology, it is required the deposition of MOFs, normally obtained in the form of powders, on solid substrates <sup>6,49</sup>. Among the types of MOFs thin films, we will focus on SURMOF (surface-supported metal-organic frameworks) fabricated using layer-by-layer (LBL) spray method, where the orientation and film thickness can be well-controlled and occur at room temperature and ambient pressure <sup>33</sup>. Searching in the literature, it is notable the conventional functionalization of the gold surface through the MHDA self-assembled monolayer (SAM) and the construction of a MOF film (SURMOF) of Cu-BTC upward. The first studies related to the MOFs association with mesoporous silica started around 2012. This demonstrates how recent this topic is and the opportunity for new discoveries <sup>51</sup>.

The fundamental SURMOF principle was exposing a substrate to dilute solutions of metal-containing for a period of time and then expose to linkers solution to grow highly oriented layer-by-layer MOFs <sup>52</sup>. In the cited spray method, (Figure 11) an aerosol is produced by expanding solutions of the reactants through a small nozzle. When the droplets of the resulting aerosol hit the substrate, the material is deposited <sup>7,33</sup>. The LPE spray method has been used due to its ability to produce thin SURMOF coatings in a short time. Using this procedure, SURMOFs were obtained with a thickness in the micrometer order in just a few hours <sup>49</sup>.

Hence, our approach relies on the optimization of the experimental parameters for the direct layer-by-layer spray deposition of Cu-BTC precursors (organic linker: BTC, metal node: copper) on the SBA-15 mesoporous silica pastilles to form CuBTC+SBA-15 SURMOF using OH-terminated groups as anchoring. The gold conventional supports were functionalized by a thiol-based SAM and the mesoporous SBA-15 silica was simply activated by water. These hybrid materials are expected to exhibit gas separation behavior and improved mechanical resistance of the MOF due to silica support <sup>53</sup>.



## 3.2 Experimental

### 3.2.1 Materials

Copper acetate anhydride ( $\text{Cu}(\text{OAc})_2$ ), 1,3,5-benzene tricarboxylic acid ( $\text{H}_3\text{BTC}$ ), ethanol (99.5%) and The methylcellulose (Methocel A4M) were obtained from Sigma-Aldrich and used as received unless otherwise stated. The SBA-15 mesoporous silica powder was previously obtained employing the established synthesis<sup>31,54,55</sup> and calcined at 500 °C.

### 3.2.2 Substrate Preparation

The Cu-BTC SURMOF membranes were synthesized on both silica and gold substrates. In the case of silica, it was prepared a mesoporous SBA-15 silica powder and then conformed in pastilles. A preparation of powder of silica was prepared by sol-gel route, based on the literature<sup>55</sup>. For the gold, the substrates (200-nm Au/2-nm Ti evaporated on Si wafers) were at first functionalized by self-assembled monolayers, SAMs, of 16-mercaptohexadecanoic acid (MHDA), that were prepared by immersing Au substrates into 20 mM ethanolic solutions for 70–72h. After removal of the samples from solution, they were rinsed with ethanol and dried in a stream of  $\text{N}_2$ <sup>7,27</sup>.

### 3.2.3 Preparation of silica (SBA-15) substrates

SBA-15 silica pastilles were prepared by mixing 1.5 g of powder of SBA-15 mesoporous silica, 0.2 g of methocel and 0.6 mL of deionized water. The solid solution was transferred to an evacuable pellet dies accessory and submitted to 500 kfg/m<sup>2</sup> pressure during three minutes. The samples were calcined at a rate of 1 °C/min from room temperature to 800 °C for 1h, to remove the methocel. The obtained silica disks were activated by immersion in deionized water under ultrasound for 10 minutes to ensure the presence of OH groups on the surface.

The OH-terminated groups are found on the silica surface in three forms: (a) isolated free silanols,  $\equiv\text{SiOH}$ ; (b) geminal free silanols (or silanediols)  $\equiv\text{Si}(\text{OH})_2$ ; (c) vicinal, H-bonded or bridged silanol groups. When these OH groups come into contact with the water, they act as centers of adsorption and the hydroxylated regions are gradually expand, until eventually the entire surface become hydroxylated <sup>56</sup>. This explains why gold functionalized surfaces may be replaced by SBA-15 water activated pastilles.

### 3.2.4 Preparation of the metal-organic frameworks

The following procedure for the Cu-BTC deposition were the same for both substrates cited types. It was used the spray layer-by-layer (LBL) method adapted from the procedure described by Arslan and coworkers <sup>33</sup>, as shown in Figure 11. These substrates were then placed on a sample holder (Figure 11a) and subsequently sprayed with a 1 mM of  $(\text{Cu}(\text{OAc})_2)$  ethanol solution (Figure 11b) for 10 seconds and then with a 0.2 mM of  $\text{H}_3\text{BTC}$  solution (Figure 11c) for 20 seconds at room temperature. Typical values of spray parameters were employed, such as, gas pressure of 1.5 psi, and distance between the nozzle and the target of 0.1 m, based on the literature <sup>7</sup>. Between each step the substrates were manual rinsed with ethanol. Through the number of cycles, the thickness of the SURMOF can be controlled. We work with 20 deposition cycles to obtain SURMOF layers. After the complete deposition, the sample was removed from the sample holder, washed with ethanol, and dried with  $\text{N}_2$ .

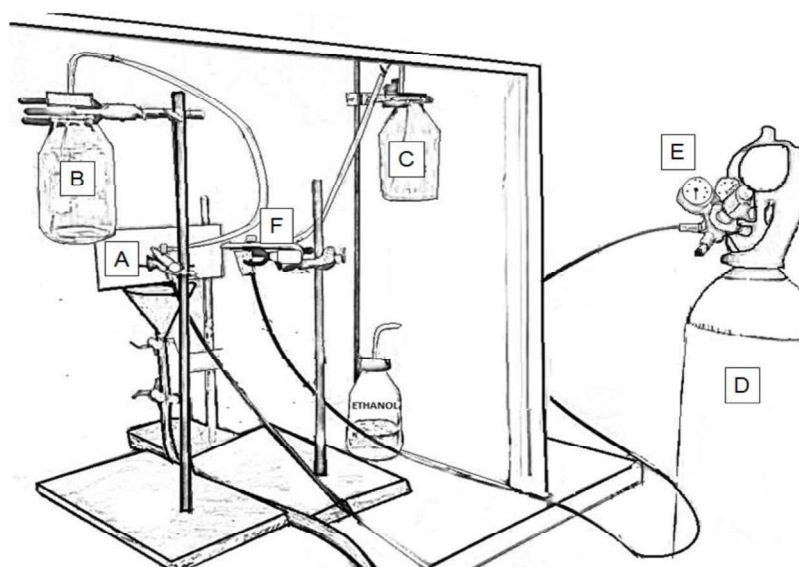


Figure 11. Schema of simple spray method employed for the fabrication of MOF thin films: (a) sample holder, (b,c) solutions containers, (d) gas supply, (e) gas flow controller, (f) dosing valves

### 3.2.5 Characterization

The materials were characterized by powder X-ray diffractometer (XRD) PANalytical Empyrean X-ray in the  $2\theta$  range from  $5^\circ$  to  $20^\circ$ , using scan speed of  $0.02^\circ$  with an acquisition time of 20s per step. FTIR spectroscopy (Perkin-Elmer Frontier spectrometer with aid of VARS accessory) was performed between  $4000\text{ cm}^{-1}$  and  $400\text{ cm}^{-1}$ , with a resolution of  $4\text{ cm}^{-1}$  and 128 scans. Scanning electron microscope (SEM) Quanta 3D FEG FEI was used for morphologies analyses. To perform the analysis on the SEM, the samples were powdered and their surfaces were covered with a layer of about 15 nm of amorphous carbon to improve surface conductivity, avoiding the accumulation of charges during image acquisition. TEM images were obtained from Transmission Electron Microscope G2-20-SuperTwin FEI microscope.

### 3.3 Results and Discussion

The surface mounted metal-organic-frameworks (SURMOF) were carried out by using SBA-15 silica, previously synthesized at Laboratory of Ceramic Materials (LMC), and silicon wafer coated with gold as substrates. Figure 12 illustrated the comparison between the surfaces before and after the deposition of Cu-BTC, where Figure 12a shows the substrate of SBA-15 silica and Figure 12b shows the substrate of SBA-15 silica after deposition of Cu-BTC, bluish surface. The noted color of the silica substrate was characteristic of the formation of Cu-BTC. In the case of gold substrate, the Figure 12c shows the MHDA-SAM without Cu-BTC and Figure 12d the MHDA-SAM with Cu-BTC.

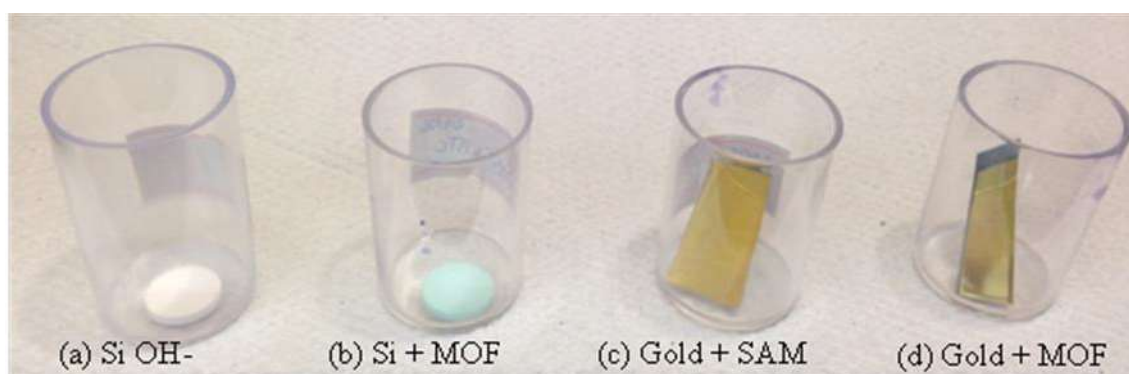


Figure 12. Illustration of (a) activated SBA-15 silica. (b) activated SBA-15 silica with Cu-BTC deposition. (c) gold with MHDA-SAM. (d) gold with MHDA-SAM and Cu-BTC deposition.

#### 3.3.1 XRD

The Figure 13 shows the XRD patterns of the resulting MOFs obtained by using layer-by-layer spray method. We compare XRD data for Cu-BTC SURMOF prepared using 20 cycles on activated SBA-15 silica substrate (Figure 13a) with a typical data for Cu-BTC SURMOF fabricated on functionalized gold conventional substrate (Figure 13b). The XRD patterns demonstrated the success of the adapted spray method and that MOF material has been deposited on SBA-15 silica substrate. The gold functionalized with COOH-terminated substrate, presented the growth of  $[\text{Cu}_3(\text{BTC})_2]$  along the [200]

direction. On the other hand, the OH-terminated SBA-15 silica surface presented MOF-layers with a [222] orientation. These results using SBA-15 OH-terminated substrate corroborate the researches conducted with others anchoring organic reagents, such as 11-mercaptoundecanol (MUD), which presented the growth in the same [222] direction <sup>32</sup>. In addition, the SBA has amorphous walls that do not appear in the DRX, which further proves that the peak presented refers to the built MOF. Thus the different substrate termination controls the growth direction of the MOF. The FTIR results indicated the formation of a Cu-BTC SURMOF on SBA-15 silica supports, which is consistent with results obtained from XRD.

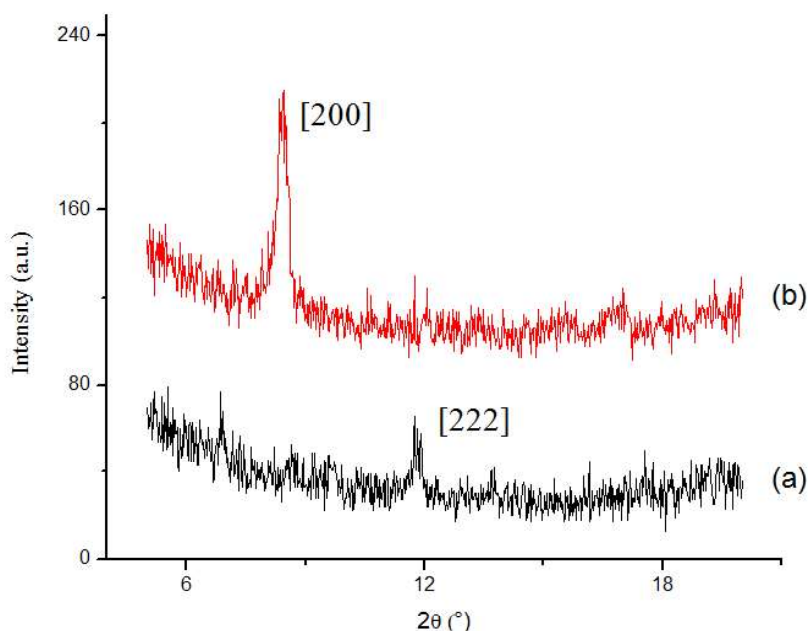


Figure 13. Out-of-plane data for Cu<sub>3</sub>(BTC)<sub>2</sub> (a) growth on OH- activated SBA-15 silica substrate and (b) growth on MHDA SAM on gold substrate.

### 3.3.2 FTIR

The FTIR spectrum illustrated in Figure 14 shows the comparison between the synthesized Cu<sub>3</sub>(BTC)<sub>2</sub> on MHDA-SAM on gold substrate (Figure 14.a), Cu<sub>3</sub>(BTC)<sub>2</sub> on OH-terminated SBA-15 mesoporous silica (Figure 14.b) and powder of SBA-15 mesoporous silica (Figure 14.c). For Cu<sub>3</sub>(BTC)<sub>2</sub> (Figure 14a),

the peaks at  $1652\text{ cm}^{-1}$  and  $1384\text{ cm}^{-1}$  were respectively attributed to the asymmetric and symmetric stretching vibrations of C=O existing in the BTC ligands<sup>8</sup>. For the SBA-15 (Figure 13c), the main bands are from  $1300$  to  $1000\text{ cm}^{-1}$ , due to Si-O-Si asymmetric stretching vibrations<sup>31</sup>. The characteristic vibrational band related to the Si-OH groups was seen around  $982\text{ cm}^{-1}$ <sup>8</sup>. As presented in Figure 13b, it was found that the FTIR spectra of the synthesized Cu-BTC SURMOF on OH-terminated SBA-15 silica substrate presented the peaks of Cu-BTC on gold substrate. Furthermore, the OH functional groups appeared in the FTIR spectra of pure SBA and then decreased in the peak of OH in the MOF + SBA suggesting a decreasing of available OH on the silica surface and the MOF adhesion to the surface of the support, which corroborates the results of XRD. This shows that the OH-terminated groups bind to the MOF and assisted in the orientation of its structure.

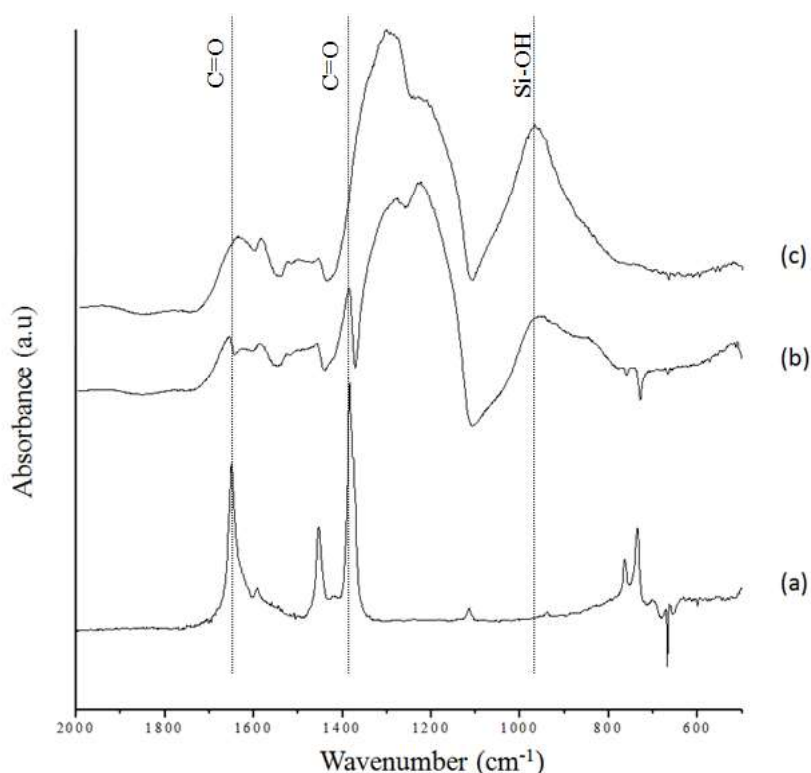


Figure 14. FTIR spectra of (a) Cu-BTC on gold substrate, (b) Cu-BTC on SBA-15 silica substrate and (c) SBA-15 silica

### 3.3.3 SEM and TEM

The SEM and TEM images shown in Figure 15 demonstrated the morphologies of the  $\text{Cu}_3(\text{BTC})_2$  prepared by using spray layer-by-layer method. The Figure 15a presents the formation of the homogeneous pastille of pure SBA-15 silica. Some research has been done to recover silica substrates with SURMOF without much success<sup>57</sup>. As shown in the SEM images in Figure 15b, in this work we achieve an homogeneous distribution of the Cu-BTC SURMOF film on SBA-15 silica pastilles and proved the success of the LBL spray method to prepare this coating on silica supports without any organic functionalization. Figure 15c showed the Cu-BTC SURMOF on conventional gold substrate functionalized with the COOH organic group, by using MHDA-SAM. The Figure 15d presents the regular octahedral morphology of Cu-BTC with a size around 150 nm growth on gold with MHDA-SAM substrate. In the Figure 15e it was observed the highly ordered mesoporous structure of original SBA-15. On the other hand, Figure 15f suggested the phase distributions of Cu-BTC crystals on SBA-15. It is possible to observe the regular arrangement of MOF forms interacting with the SBA-15 substrate. Furthermore, the Cu-BTC nanocrystals were attached on SBA-15 silica substrate and grew along the direction under silica influence due to the presence of OH-terminated group. These results were in line with the findings from the FTIR and XRD measurements and demonstrated that the room temperature layer-by-layer spray method is well-suited for the growth of such MOF thin film on mesoporous supports.



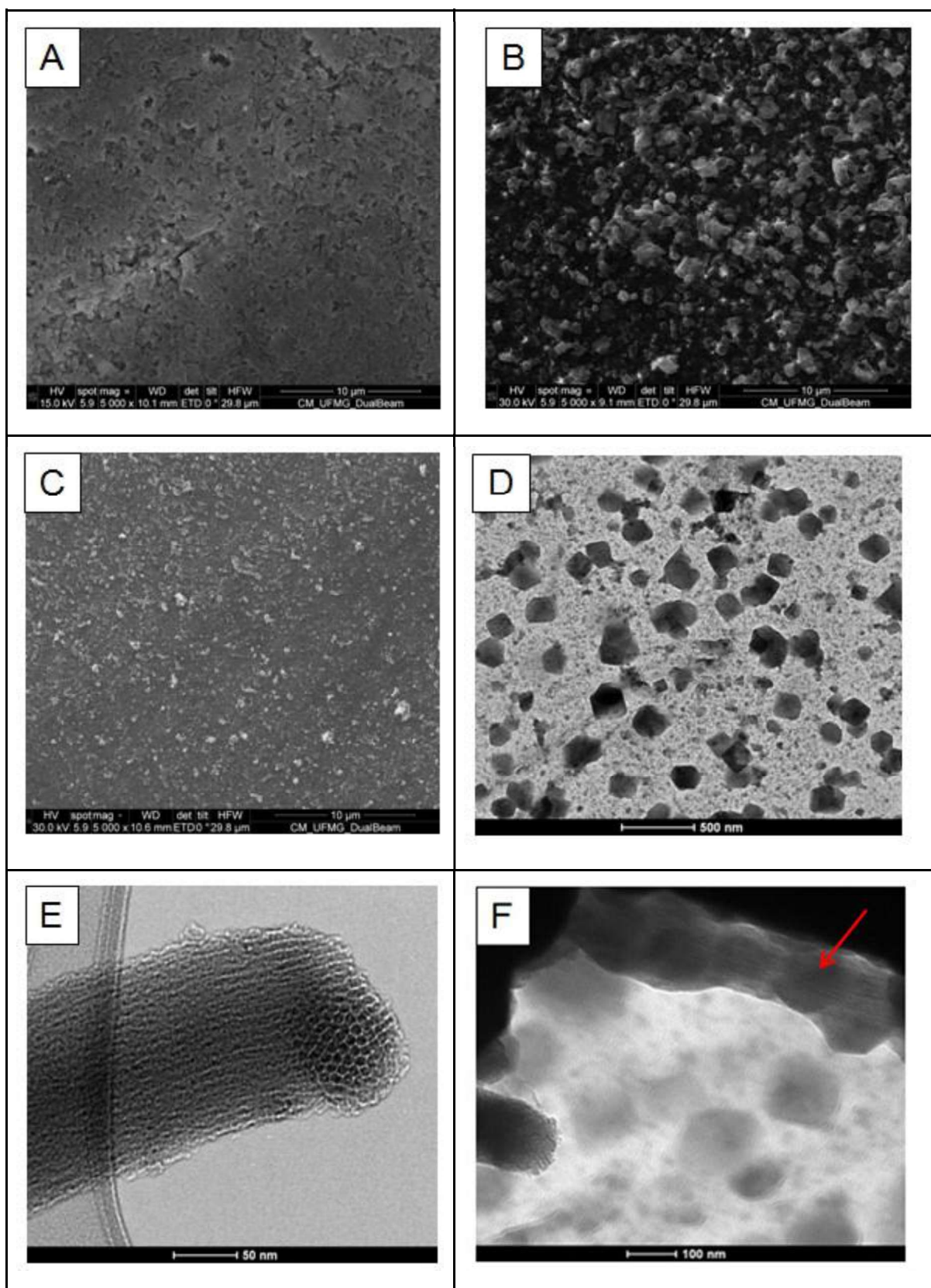


Figure 15. SEM images of (a) SBA-15 pastille, (b) SBA-15 + Cu-BTC by LBL spray method, (c) gold substrate + MHDA-SAM + Cu-BTC and TEM images of (d) gold + MHDA SAM + Cu-BTC (e) SBA-15 silica and (f) SBA-15 + Cu-BTC by LBL spray method



### **3.4 Conclusions**

In conclusion, we have successfully synthesized and characterized a Cu-BTC MOF on mesoporous SBA-15 silica substrate by using a new approach of the layer-by-layer spray method. The obtaining of SBA-15 pastilles and its simple activation with water was enough to provide the necessary OH-terminated groups to anchor the MOF on the silica surface. The chosen method, besides allowing the formation of MOF at room temperature and ambient pressure, allowed the oriented growth of the structure, as confirmed by instrumental analysis. Therefore, this work contributes significantly to the recent studies related to the synthesis of SURMOF on mesoporous materials. The pastilles were sent to Germany to evaluate the performance as gas separation membranes. Studies are still ongoing.

## **CHAPTER 4. Production of rod-like morphology of $\text{Cu}_3(\text{BTC})_2$ metal-organic frameworks using one minute sonication**

### **Abstract**

This paper reports a new short time strategy for producing rod-like morphology of metal-organic frameworks (MOFs), by using one minute ultrasonic homogenizer (or “sonicator”) at room temperature and ambient pressure. The crystallinity of the obtained  $\text{Cu}_3(\text{BTC})_2$  was investigated by X-ray diffraction and its stable formation corroborated with Fourier transform infrared spectroscopy (FTIR) results. This study promotes an optimization process to synthesize MOFs.

Keywords: metal-organic frameworks, ultrasonic energy, morphology

### **4.1. Introduction**

Metal-organic frameworks (MOFs) are crystalline and porous materials with chemical flexible properties which are composed of transition metals ions or clusters linked by organic ligands<sup>5,45</sup>. They present wide applications, such as gas storage and separation<sup>6,39,58</sup>, catalysis<sup>59</sup>, carbon dioxide capture<sup>9</sup>, among others<sup>3,60</sup>. In this sense, researches have been done to improve its synthesis parameters<sup>61,62</sup>. The metal-organic framework  $\text{Cu}_3(\text{BTC})_2$ , a coordination compound formed by copper and trimesic acid, also known as Cu-BTC and HKUST-1, is one of the widely studied MOF.

Several methods are applied in Cu-BTC synthesis, such as sonochemical, solvothermal, electrochemical and microwave<sup>48</sup>. The sonochemical procedure, in particular, has been noted in the last years<sup>63,64</sup>, although some ultrasonic machines offer dispersed energy, which difficult the synthesis of the material<sup>65,66</sup>. This suggests the necessity to discover new routes to achieve an increase

in the yield of produced MOFs and reductions of the synthesis time. In this scenario, the sonicator has been recently used to obtain the Cu-BTC MOF and varied morphologies<sup>67–69</sup>. In this study, we produced a rod-like Cu-BTC and presented an optimized synthesis through ultrasonic homogenizer (or “sonicator”).

## **4.2. Experimental**

### **4.2.1 CuBTC preparation**

The  $\text{Cu}_3(\text{BTC})_2$  DMF-based was prepared using copper acetate anhydride ( $\text{Cu}(\text{OAc})_2$ ), 1,3,5-benzene tricarboxylic acid ( $\text{H}_3\text{BTC}$ ), and ethanol (99.5%), used without further purification. All the reagents were purchased by Sigma-Aldrich. The  $\text{H}_3\text{BTC}$  was dissolved in 25 mL N,N-dimethylformamide (DMF 99,8%) and cupric acetate was added in the same solution. Then ultrasonic irradiation was applied at different reaction times. The mixture was filled in a 50 mL vessel and heated to 120 °C for 12 h, within and without autoclave to compare. The products were filtered, washed with ethanol and dried at 60 °C.

### **4.2.2 Ultrasonic radiation interference experiments**

During the ultrasonic irradiation cited step, the reaction times were varied from 1 min to 60 min at a frequency of 24 KHz and 60% of power (UP 200S, Hielscher Ultrasonics GmbH, Teltow, Germany), called in this work “sonicator”, output 200W, Figure 16, Sonotrode S3. The time was varied to find the necessary minimum time to obtain the material.

### **4.2.3 Techniques used for characterization**

The materials were characterized by powder X-ray diffractometer (XRD) PANalytical Empyrean X-ray in the  $2\theta$  range from 5° to 20°, using scan speed of 0.02° with an acquisition time of 20s per step. Due to the anisotropic shape of the particles, preferential orientation was checked with the help of the Williamson-Hall approach<sup>70</sup>. FTIR spectroscopy (Perkin-Elmer Frontier spectrometer with aid of

ATR accessory) was performed between  $4000\text{ cm}^{-1}$  and  $400\text{ cm}^{-1}$ , with a resolution of  $4\text{ cm}^{-1}$  and 128 scans. Scanning electron microscope (SEM) Quanta 3D FEG FEI was used for morphologies analyses. To perform the analysis on the SEM, the samples were powdered and their surfaces were covered with a layer of about 15 nm of amorphous carbon to improve surface conductivity, avoiding the accumulation of charges during image acquisition. TEM images were obtained from transmission electron microscope G2-20-SuperTwin FEI microscope. Thermal analyses (TGA) were measured using a Perkin-Elmer STA 6000 simultaneous thermal analyzer Instrument in  $\text{N}_2$  atmosphere. The materials were heated from  $30\text{ }^\circ\text{C}$  to  $900\text{ }^\circ\text{C}$  at a rate of  $10\text{ }^\circ\text{C}/\text{min}$ .

### 4.3 Results and discussion

In this study we use an ultrasonic homogenizer (or “sonicator”) that works both directly through cavitation energy transfer mechanism, whereby bubbles form and collapse, as well as through the ultrasonic forces, by introducing a probe into the sample, as shown in Fig. 16. The probe vibrates rapidly and transfers its ultrasonic energy to the sample with a more localized process, which provides uniform MOFs in just a few seconds<sup>63,65,66</sup>.

Ultrasound is cyclic mechanical vibration between 20 kHz and 10 MHz. It can interact with liquids, alternating areas of compression (high pressure) and rarefaction (low pressure). In the low pressure region small bubbles are formed. The bubbles grow (tens of micrometers) under alternating pressure and ultrasonic energy is accumulated. When the bubbles reach their maximum size, they become unstable and collapse: cavitation process. Rapid energy release with heating and cooling rates of  $10^{10}\text{ K/s}$ , temperatures around 5000 K and pressures of around 1000 bar. Thereby, these points present very unusual conditions of short duration and extremely high temperatures and pressures inside the collapsing bubble and nearby (ring of  $\pm 200\text{ nm}$ )<sup>26</sup>.

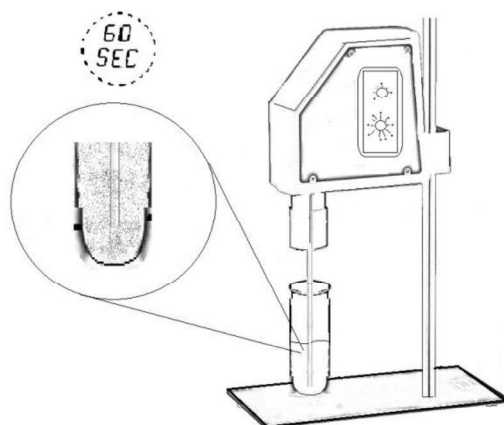


Figure 16. Illustration of the dispersion of nanoparticles by using high energy ultrasonic homogenizer to MOF preparation

In this way, the Cu-BTC MOFs were prepared by using copper acetate and  $H_3BTC$  in DMF under sonicator for only 1 min, at room temperature and ambient pressure, (Figure 17a) which was enough to obtain a high amount of  $Cu_3(BTC)_2$  (68,5%, based on Cu). Furthermore, combining with the solvothermal method, by using autoclave, we achieved even higher values of  $Cu_3(BTC)_2$  (78,1%, based on Cu), Figure 17b and after the drying process Figure 17c.

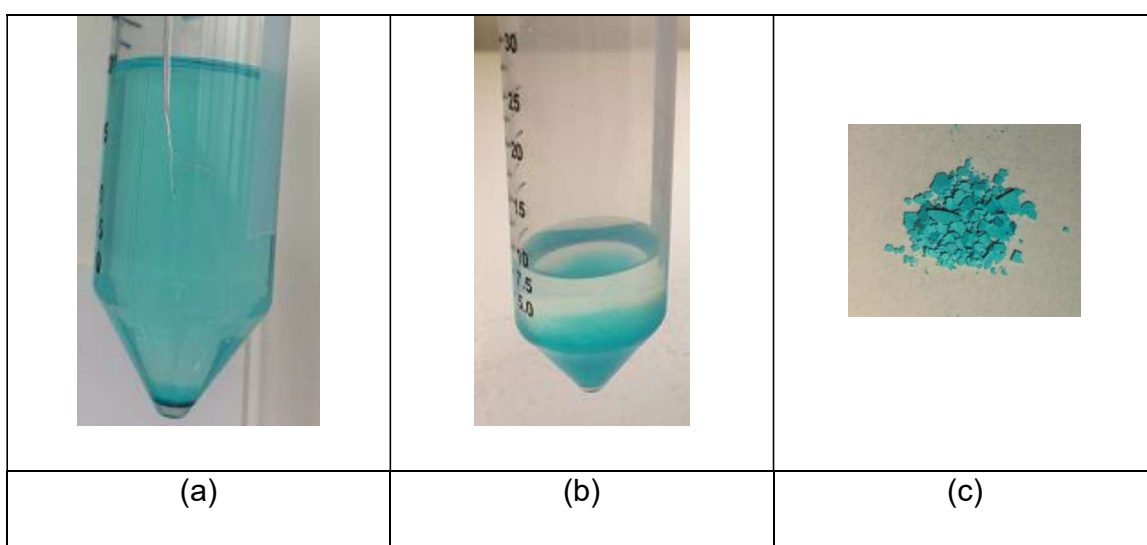


Figure 17. Process of obtaining MOFs: (a) mixture of copper and BTC precursors, (b) separation of the two phases (MOF and solvent) characteristic of the formation of the MOF and (c) final MOF powder.

### 4.3.1 XRD

The Figure 18 shows the XRD patterns of the resulting MOFs obtained by using sonicator even at very low times. The results for the samples obtained using one and five minutes of sonication were evaluated and compared with the literature. In this sense, all of the diffraction peaks could be correlated to the crystalline  $\text{Cu}_3(\text{BTC})_2$  pattern (ref.<sup>21,71</sup>). The absence of additional peaks in the presented range demonstrates a satisfactory level of purity of the crystalline structure. In addition, reflections of an unknown phase appear (not shown here) when the reaction time was increased to 30 min, 60 min and 120 min, indicating that the structure of the sample is changed due to ultrasound irradiation for a long reaction time, as suggested by the results for the five minutes sample shown at Figure 17. Furthermore, the yield of solvent into the MOF pores may interfere in the relative intensities of the diffraction peaks<sup>63,66</sup>. From the Williamson-Hall plot applying all observed (hkl)-reflections, no anisotropy could be deduced. Thus, the shape of the particles is not reflected in the crystalline domains. Their size was calculated from the plot to 23 nm and the stress/strain parameter  $\epsilon_0$  to 0.0021  $d_0/d$ , with  $d$  the lattice plane distance. These results indicated that fast sonicator dispersion of the particles allows the formation of crystalline and well-defined structures, which is consistent with results obtained from FTIR.

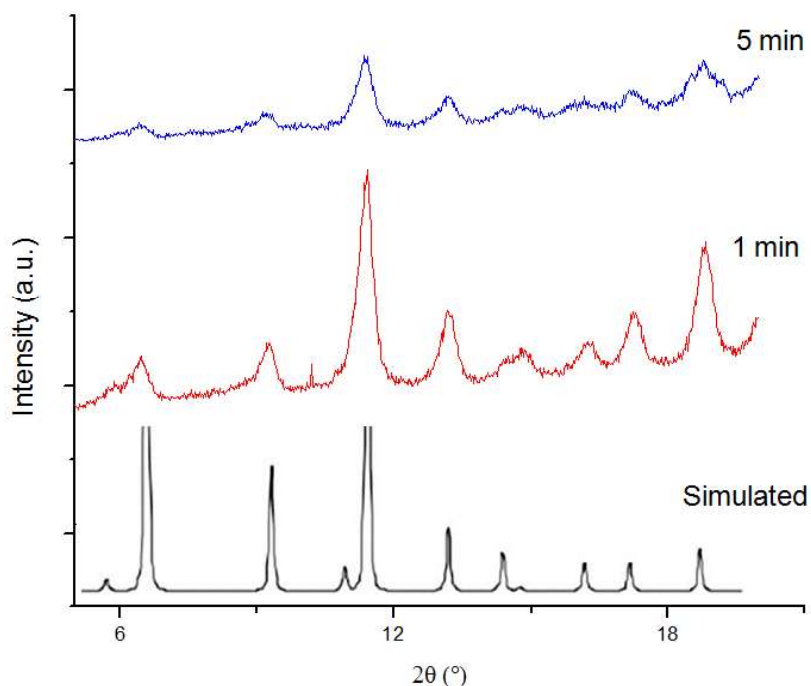


Figure 18. Powder X-Ray diffraction patterns simulated from the crystallographic data of  $\text{Cu}_3(\text{BTC})_2$  (ref. <sup>71</sup>), and samples synthesized by using high energy sonicator: 1 min and 5 min.

#### 4.3.2 FTIR

The FTIR spectrum illustrated in Figure 19 shows the comparison between the synthesized  $\text{Cu}_3(\text{BTC})_2$  and  $\text{H}_3\text{BTC}$ , source of BTC. The bands around  $1634\text{ cm}^{-1}$ ,  $1446\text{ cm}^{-1}$ ,  $1419\text{ cm}^{-1}$  and  $1372\text{ cm}^{-1}$  refer to the pure Cu-BTC which are attributed to vibrations of its carboxylate group. The  $1634$  and  $1419\text{ cm}^{-1}$  founded bands were attributed to asymmetric  $\nu_s(\text{COO})$  and symmetric  $\nu_s(\text{COO})$  stretching modes, respectively. These modes can be assigned to those carboxylate groups located in the big pores of Cu-BTC. Meanwhile, the  $1446$ , and  $1372\text{ cm}^{-1}$  peaks were attributed to asymmetric  $\nu_s(\text{COO})$  and symmetric  $\nu_s(\text{COO})$  stretching vibrations of those carboxylate groups located in the smaller pores <sup>8,69,72</sup>.

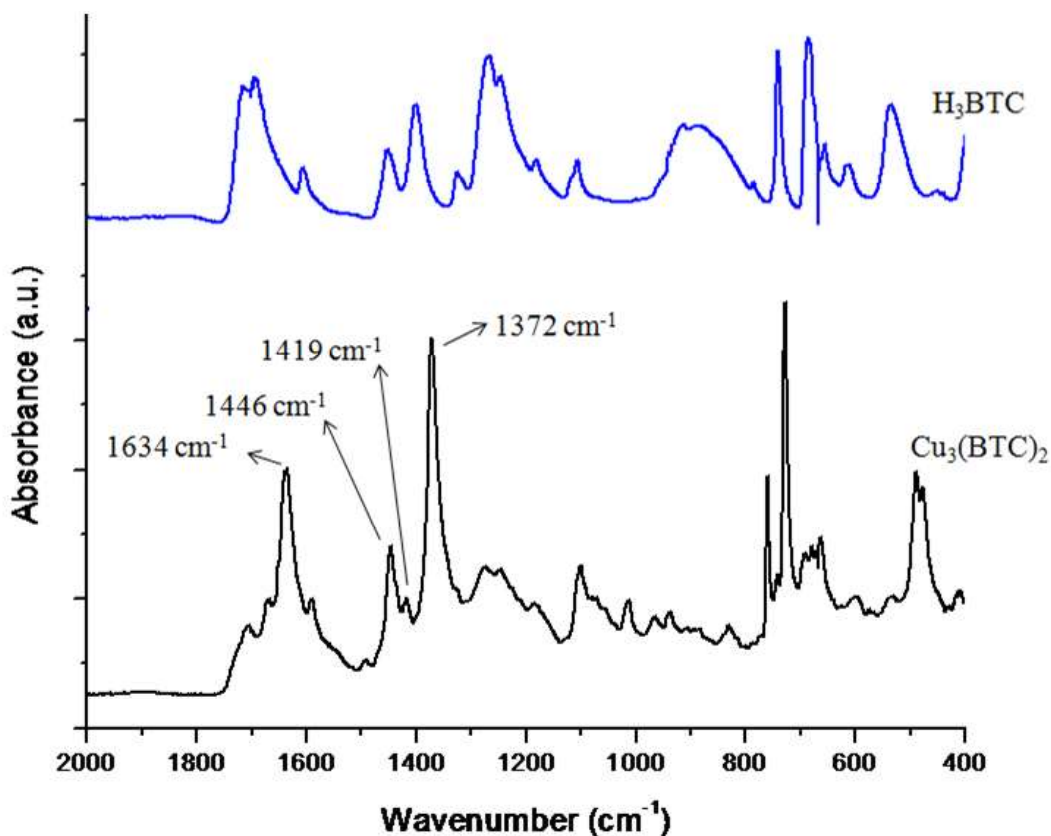


Figure 19. FTIR spectrum of H<sub>3</sub>BTC and Cu<sub>3</sub>(BTC)<sub>2</sub> sample synthesized by 1 min ultrasonic homogenizer

#### 4.3.3 Thermogravimetric analysis TG/Degradation

The obtained material was studied in terms of thermal stability by using TG/DTG analysis. The curves of Cu-BTC are shown in Figure 20. The first region showed a weak peak around 100 °C which was related to the small presence of water that was physically adsorbed in the pores. The second region about 150 °C suggests the loss of residual DMF and ethanol solvents. The third region of weight loss occurred around 330 °C, may be associated with the decomposition of the BTC ligands and secondary building units in Cu-BTC, which indicates a complete collapse and degradation of the MOF structure.



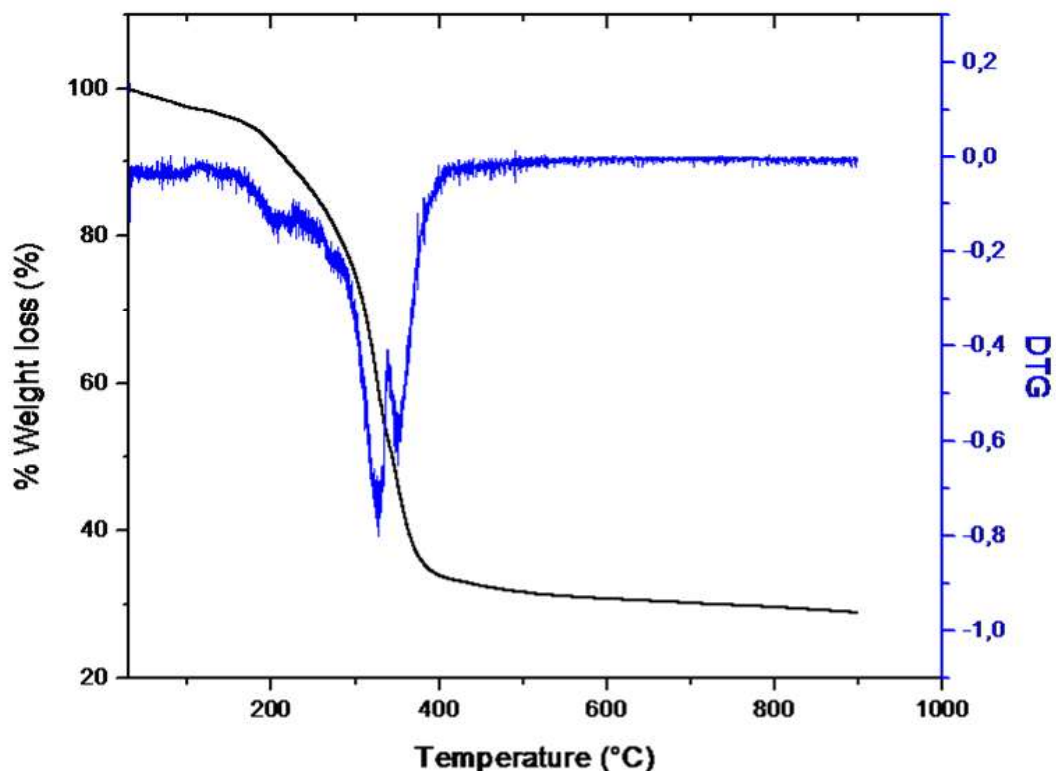


Figure 20. TG/DTG of  $\text{Cu}_3(\text{BTC})_2$  sample synthesized with ultrasonic homogenizer

#### 4.3.4 SEM and TEM

The SEM and TEM images shown in Figure 21 demonstrated the morphologies of the  $\text{Cu}_3(\text{BTC})_2$  prepared by using 1 min sonication method. The morphologies features of rod-likes are shown in Figure 21a, with a size range of 1–2  $\mu\text{m}$ . According to the literature, the conventional solvothermal method presented MOFs with octahedral shape and crystal sizes in the order of nanometers, which were smaller than those found here<sup>63,73</sup>. The crystal size can also be tuned through the reaction conditions. When the reaction was conducted using the same sonication process, although at ambient pressure, Figure 21b, the rod-likes appeared more agglomerated, suggesting the formation of interconnected hollow regions. Figure 21c and d well indicated the crystalline nature of the nanomaterials by transmission electron microscope (TEM). These images corroborated the morphologies presented above with a size around 1.4  $\mu\text{m}$ , and exhibited the regular rod-like morphology with hexagonal-shaped

transversal section with the diameter around 100 nm, respectively. This indicated that using even few seconds of homogenizing ultrasonic irradiation, the rod-like morphology of Cu-BTC can be achieved and modeled.

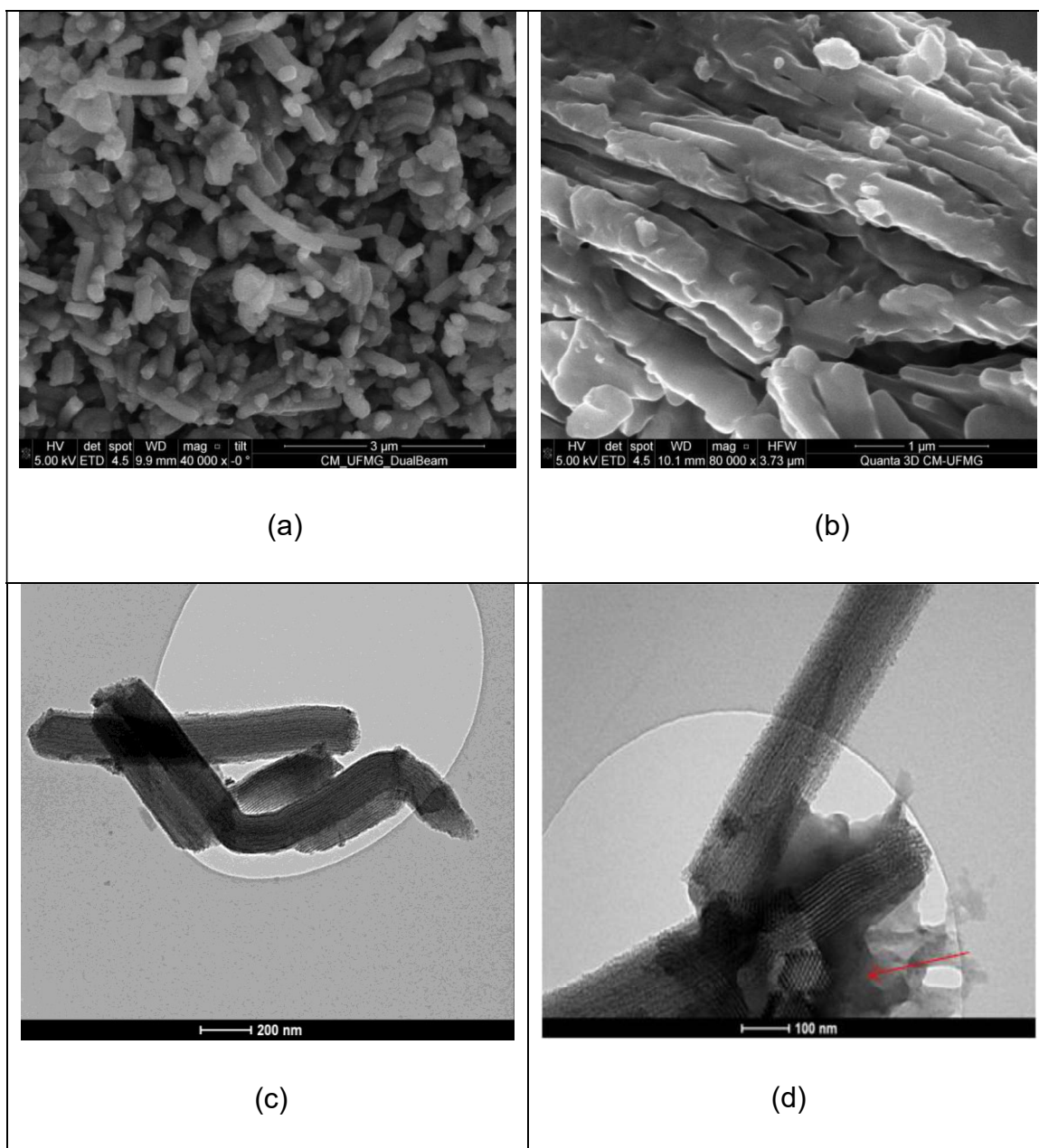


Figure 21. SEM images of Cu-BTC by one minute ultrasonic irradiation homogenizer under different pressures (a) autoclave, (b) ambient pressure; and TEM images of Cu-BTC by one minute ultrasonic irradiation homogenizer both (c) and (d) under autoclave.

#### **4.4 Conclusions**

In summary, the obtained results in this study confirmed the successful rapid ultrasonic homogenization technique to rod-like  $\text{Cu}_3(\text{BTC})_2$  formation. The material could be prepared by using one minute sonication method due its rapidly probe vibration and the ultrasonic energy transference. This more localized process provided uniform MOFs even at room temperature and ambient pressure. In addition, the studied homogenization step promoted an optimization process of the MOF synthesis and could be associated with the as solvothermal and sonochemical conventional methods.

## **CHAPTER 5. Syntheses of environmentally-friendly Cu-BTC metal-organic frameworks with unusual morphology and potential to CO<sub>2</sub> capture**

### **Abstract**

MOFs consist of organic-inorganic hybrid crystalline materials where a metal is linked by coordination bonds to organic ligands. They exhibit high surface areas, large free volumes, and changeable pore sizes. Its structure can be modified depending on the required properties. This study demonstrates the development of a water-based Cu-BTC with an unusual morphology, in different Cu/BTC ratios with CO<sub>2</sub> capture potential. The MOF particles were synthesized via *in situ* crystallization method. They were characterized as their crystallinity and uniformity using X-ray diffraction, FTIR spectroscopy, scanning electron microscopy and scanning probe microscopy. The CO<sub>2</sub> capture capacity was evaluated by thermogravimetric analysis. It was obtained a water-based Cu-BTC which has high CO<sub>2</sub> adsorption capacity at room temperature and ambient pressure and the material was also found to exhibit repeatability during 3 cycles of adsorption/desorption.

Keywords: metal-organic framework, carbon dioxide, thermogravimetric analysis, adsorption and desorption cycles.

### **5.1. Introduction**

In recent years, concern for the gas pollution resulting from anthropogenic emissions has been gaining ground due to CO<sub>2</sub> contributions to global problems such as release of toxic gases and greenhouse gases. This has led to a growing scientific consensus that postulates CO<sub>2</sub> to be the predominant cause of global climate change. Considerable efforts have therefore been made to develop environment friendly technologies for CO<sub>2</sub> capture, including absorption and adsorption of the gases<sup>42</sup>.

In this sense, the new class of crystalline and porous materials: metal-organic frameworks (MOFs) has obtained interest by researchers due to its chemical flexible properties <sup>62</sup>. Currently there are several studies related to the CO<sub>2</sub> capture and development of materials showing the efficiency of the MOFs. They adsorb about 30% CO<sub>2</sub> per cycle at ambient pressure and temperatures, reaching up 90% adsorption under high pressure and temperature conditions <sup>33,74–76</sup>.

Cu<sub>3</sub>(BTC)<sub>2</sub>, or (HKUST-1), was one of the most extensively studied MOF materials. These materials can be synthesized in various solvents. An interesting and environmentally friendly approach is to use water as a solvent to form the structures. In this context, the combination of the properties acquired by the synthesis of the nanostructured metal-organic frameworks (MOFs), object of this work, such as crystallinity, porosity and metal-ligand interactions, combined to the new applications derived from the variation of the synthesis parameters appear as an interesting alternative to reach properties at nanoscale <sup>1,2</sup>.

In this scenario, new studies have been deepening to understanding the interference of the composition and the proportion of the reagents in MOF properties <sup>67,68,77</sup>. In this study, we produced a water-based Cu-BTC with unusual morphology, in different Cu/BTC ratios with CO<sub>2</sub> capture potential, and the materials were characterized.

## **5.2. Experimental**

### **5.2.1 Cu-BTC H<sub>2</sub>O based preparation**

The Cu<sub>3</sub>(BTC)<sub>2</sub> H<sub>2</sub>O-based was prepared using copper acetate anhydride (Cu(OAc)<sub>2</sub>), 1,3,5-benzene tricarboxylic acid (H<sub>3</sub>BTC), and ethanol (99.5%), used without further purification. All the reagents were purchased by Sigma-Aldrich. The H<sub>3</sub>BTC was dissolved in 15 mL ethanol and stirred for 30 minutes.

Cupric acetate was dissolved in 10 mL water and added in the same H<sub>3</sub>BTC solution. Then the new solution was stirred again for 30 minutes. The mixture was filled in a 50 mL vessel and heated to 120 °C for 12 h using autoclave. The products were filtered, washed with ethanol and dried at 60 °C <sup>78</sup>.

### 5.2.2 Techniques used for characterization

The materials were characterized by powder X-ray diffractometer (XRD) PANalytical Empyrean X-ray in the  $2\theta$  range from 5° to 20°, using scan speed of 0.02° with an acquisition time of 20s per step. FTIR spectroscopy (Perkin-Elmer Frontier spectrometer with aid of ATR accessory) was performed between 4000 cm<sup>-1</sup> and 400 cm<sup>-1</sup>, with a resolution of 4 cm<sup>-1</sup> and 128 scans. Scanning electron microscope (SEM) Quanta 3D FEG FEI was used for morphologies analyses. To perform the analysis on the SEM, the samples were powdered and their surfaces were covered with a layer of about 15 nm of amorphous carbon to improve surface conductivity, avoiding the accumulation of charges during image acquisition. TEM images were obtained from transmission electron microscope G2-20-SuperTwin FEI microscope. Thermal analyses (TGA) were measured using a Perkin-Elmer STA 6000 simultaneous thermal analyzer Instrument in N<sub>2</sub> atmosphere. The materials were heated from 30 °C to 900 °C at a rate of 10 °C / min.

### 5.2.3 CO<sub>2</sub> uptake evaluation

The CO<sub>2</sub> adsorption performance was evaluated by carrying out Thermogravimetric analysis (TGA) and measuring the increase and decrease in weight of the samples during the sorption and desorption processes, according to procedure establish in the literature <sup>79,80</sup>. The tests were carried out with a Perkin-Elmer STA-6000 thermobalance. The samples were initially cleaned in a thermal treatment at 100 °C for 60 min, under Nitrogen flow. Subsequently, the system was cooled to a temperature of 30 °C and the CO<sub>2</sub> adsorption step was performed. The adsorption process was carried out at atmospheric

pressure, under gas flow of 50 mL/min at 30 °C for 60 min with CO<sub>2</sub> as purge gas. The cycles were performed three times to evaluate the recuperability of the material.

### 5.3 Results and discussion

In a standard procedure to prepare a Cu<sub>3</sub>(BTC)<sub>2</sub> H<sub>2</sub>O-based, the H<sub>3</sub>BTC was dissolved in 15 mL ethanol and cupric acetate in 10 mL water in two proportions of copper, Cu:BTC 1.8:1 and 1:1. Then the obtained solution was stirred for 30 minutes. The mixture (Figure 22 a) was filled in a 50 mL vessel and heated to 120 °C for 12 h using autoclave. The obtained results confirmed the successful Cu<sub>3</sub>(BTC)<sub>2</sub> formation, as shown in Figure 22 c, which were self-separated in the two phases (MOF and solvent) characteristic of the formation of the MOF (Figure 22 b) <sup>72</sup>.

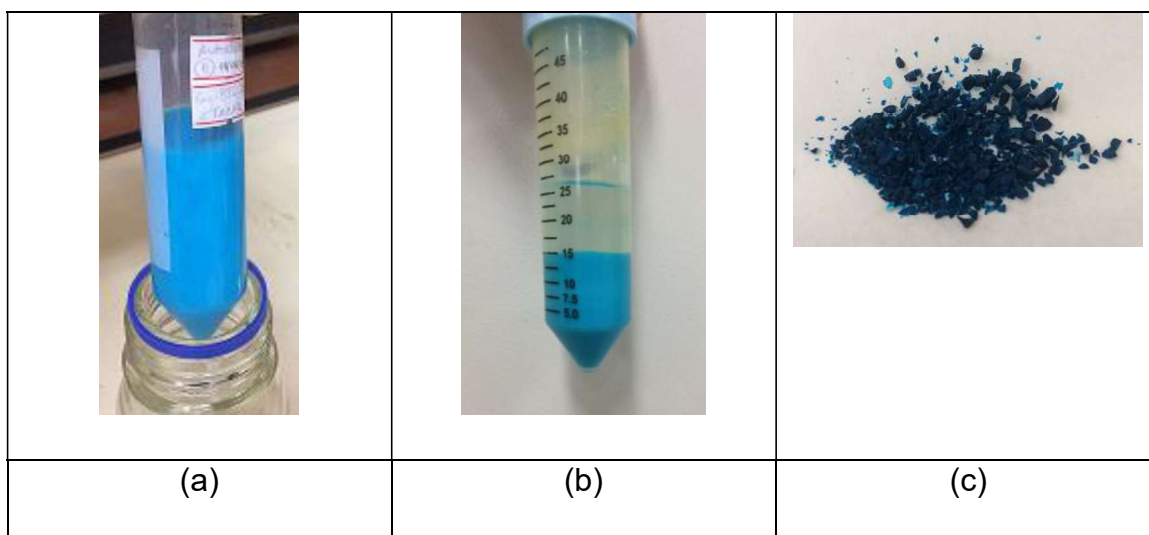


**Figure 22. Process of obtaining MOFs: (a) mixture of copper and BTC precursors, (b) separation of the two phases (MOF and solvent) characteristic of the formation of the MOF and (c) final MOF powder.**

The crystal orientation was shown by XRD and the comparison between the synthesized Cu<sub>3</sub>(BTC)<sub>2</sub> and H<sub>3</sub>BTC by using FTIR. To investigate the effect of

the Cu/BTC ratio on the morphology, we use SEM analysis. In addition, the degradation of the MOF structure under temperature and the CO<sub>2</sub> uptake were carried out by TG analysis. This last procedure allowed us to observe the MOF regenerable capacity during the CO<sub>2</sub> adsorption and desorption experiment.

### 5.3.1 XRD

The comparison of XRD patterns of obtained 1.8:1 Cu<sub>3</sub>(BTC)<sub>2</sub> ratio sample and the simulated are shown in Figure 23. This analysis reveals the reflections corresponding to the pattern of Cu-BTC MOF material. The found planes correspond to the patterns in the literature<sup>72,78</sup>, indicating the unchanged crystal structure and its orientation. In order to obtain the crystallinity of this material, the XRD were performed and corroborated very well with the SEM images.

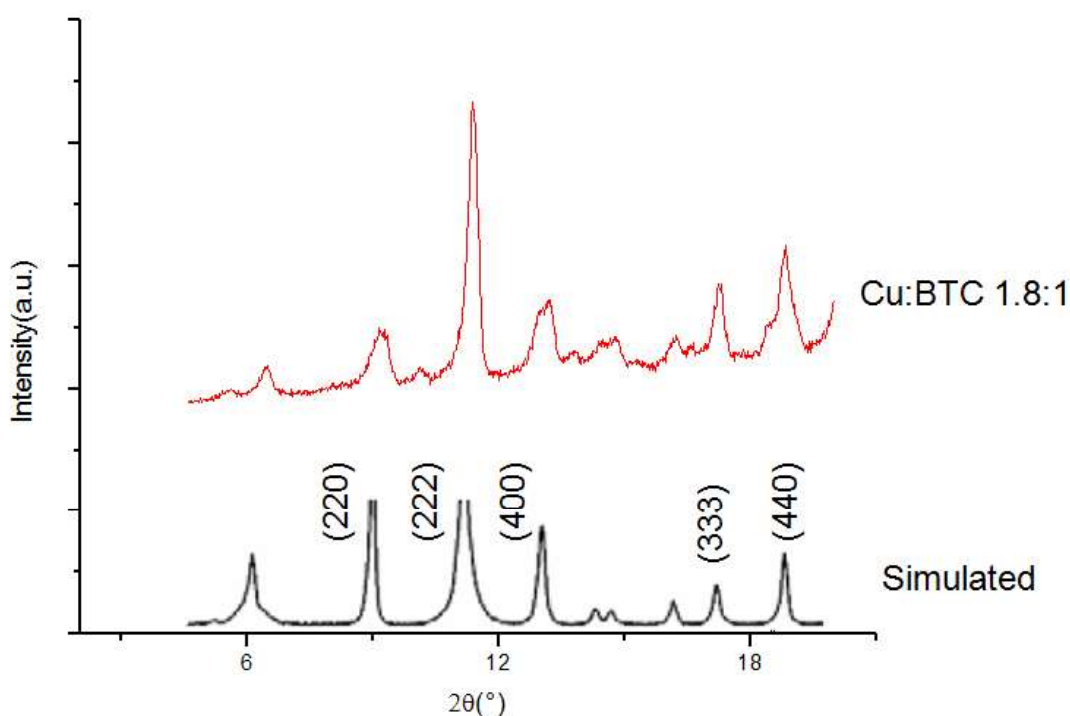


Figure 23. Powder X-Ray diffraction pattern simulated from the crystallographic data of Cu<sub>3</sub>(BTC)<sub>2</sub><sup>78</sup> (down), and synthesized sample (top).



### 5.3.2 FTIR

Figure 24 shows the FTIR spectrum of the comparison between the synthesized  $\text{Cu}_3(\text{BTC})_2$  and  $\text{H}_3\text{BTC}$ , source of BTC. From these results we observe that the bands around  $1446\text{ cm}^{-1}$  and  $1372\text{ cm}^{-1}$  refer to the pure Cu-BTC which are attributed to asymmetric  $\nu_{\text{as}}(\text{COO})$  and symmetric  $\nu_{\text{s}}(\text{COO})$  stretching modes, respectively, of its carboxylate group located in the smaller pores. The  $1647\text{ cm}^{-1}$  founded band can be assigned to the asymmetric  $\nu_{\text{as}}(\text{COO})$  carboxylate groups located in the big pores of Cu-BTC<sup>8,69,72</sup>. In addition, water can penetrate in the large pores, and it protonates the carboxylate groups<sup>69</sup>. The spectral region around  $1615\text{ cm}^{-1}$  and  $1557\text{ cm}^{-1}$  shows Cu-BTC bands related to molecular water. According to the literature, the broad band at  $1557\text{ cm}^{-1}$  is due to water coordinated with Cu in the MOF<sup>69</sup>.

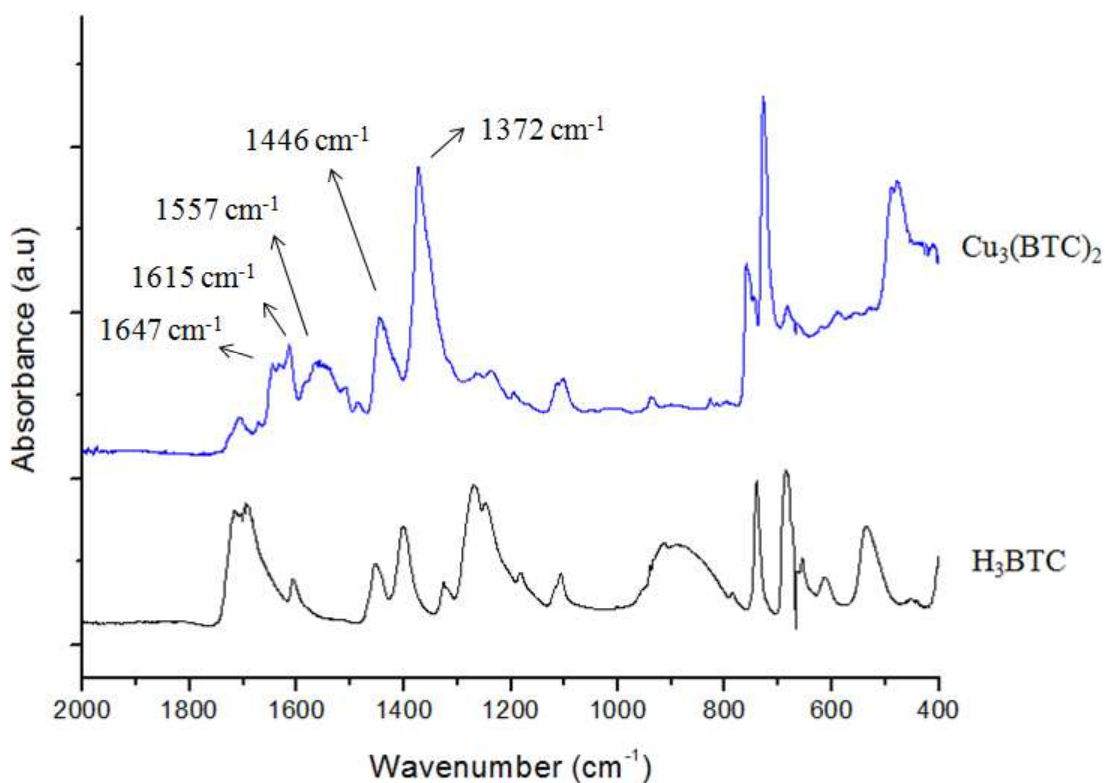


Figure 24. FTIR spectrum of  $\text{H}_3\text{BTC}$  and  $\text{Cu}_3(\text{BTC})_2$  sample synthesized

### 5.3.3 SEM and TEM

To investigate the effect of the Cu/BTC ratio on the morphology, the concentration of precursors was varied. The SEM and TEM images shown in Figure 25 demonstrated the morphologies of the  $\text{Cu}_3(\text{BTC})_2$  prepared by using different ratios of Cu and BTC. Those microscope analysis showed that the samples with the highest concentration presented the greatest roughness, while those with the lowest concentration showed smooth structures, both different from the most commonly obtained octahedron morphology<sup>26,72</sup>.

According to the literature, the ratio ligand/metal promotes a remarkable interference in the morphology of final materials. The metal presents small crystals with perfect morphology and its excess leading to building agglomerated granules, which provided unusual morphologies, such as well-defined blocks and cauliflowers<sup>77</sup>.

In the case of our study, the high ratio of copper (Figure 25 a and b) Cu:BTC 1.8:1 is constituted of interconnected granular particles of ca. 1  $\mu\text{m}$  size, forming a rough surface shown in the well-defined blocks as highlighted in the Figure 24a<sup>72</sup>. On the other hand, Figure 25c demonstrated the clear difference in morphology when decreasing the concentration. The 1:1 Cu: BTC ratio presents unusual ribbons morphology (Figure 25c). The TEM images well indicated the crystalline smooth and straight nature of the materials, which is around 5  $\mu\text{m}$  size (Figure 25d)<sup>72</sup>.

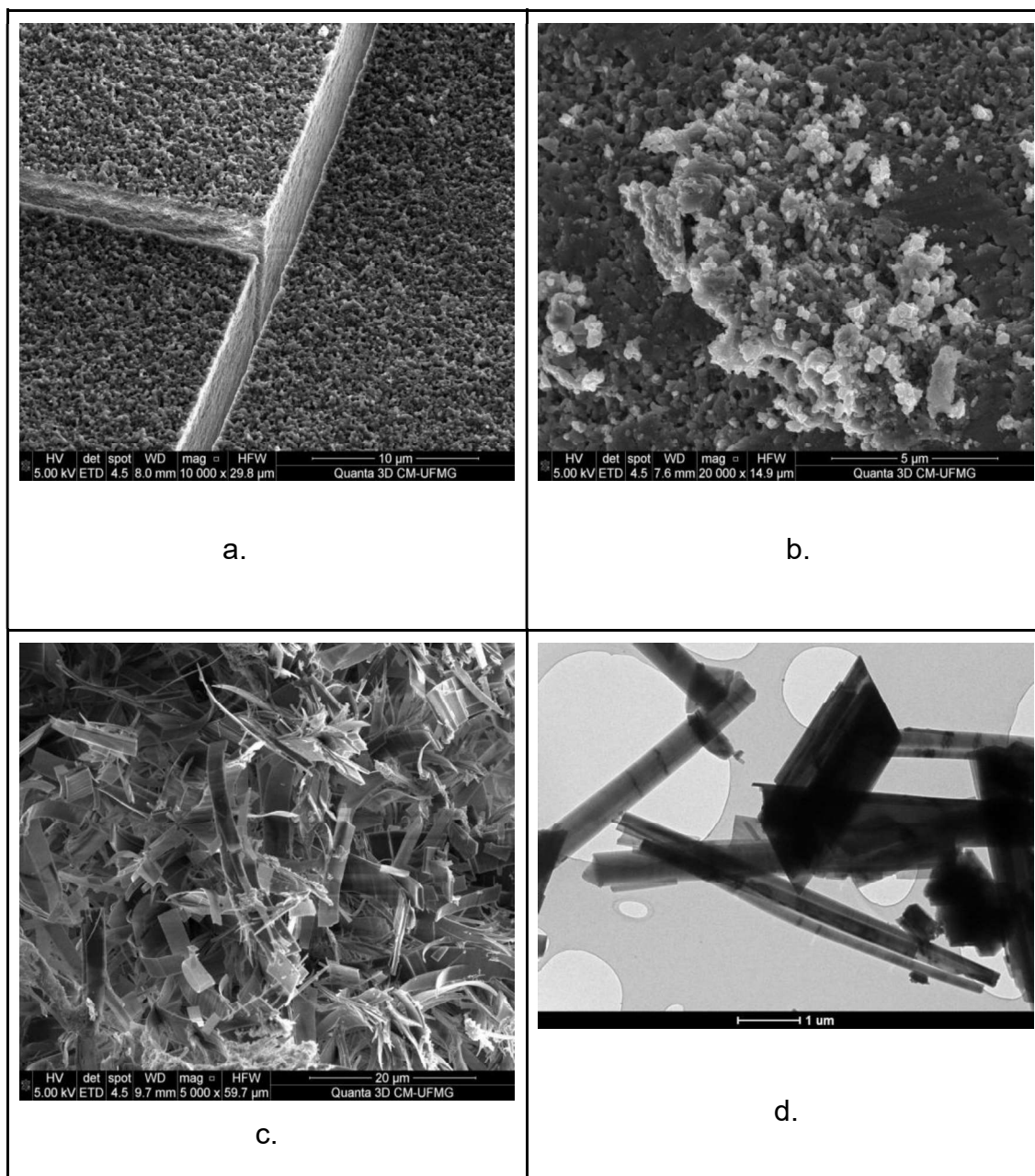


**Figure 25. SEM and TEM images illustrate how the morphologies of Cu: BTC 1.8:1 and CuBTC-1:1 change with the molar ratio between Cu and BTC. SEM images of Cu-BTC 1.8:1 ratio (a) and (b); SEM (c) and TEM (d) images of Cu:BTC 1:1 ratio.**

### 5.3.4 Thermogravimetric analysis TG/Degradation

The TG/DTG curve of the Cu:BTC 1.8:1 MOF is shown in Figure 26. There are two weight loss regions, the first step is around 25-150 °C, there was a loss of mass of 20,01 %. This may be attributed to the adsorbed water, ethanol and

hydroxyl groups<sup>43</sup>. This result is in agreement with FTIR analysis, which proves the existence of water molecules in Cu-BTC. The second weight loss region occurs at 330 °C and may be associated with the decomposition of the BTC ligands and secondary building units in Cu-BTC, which indicates a complete collapse and degradation of the MOF structure<sup>45,81</sup>. This test shows the MOF samples may be used safely at temperatures lower than 300 °C.

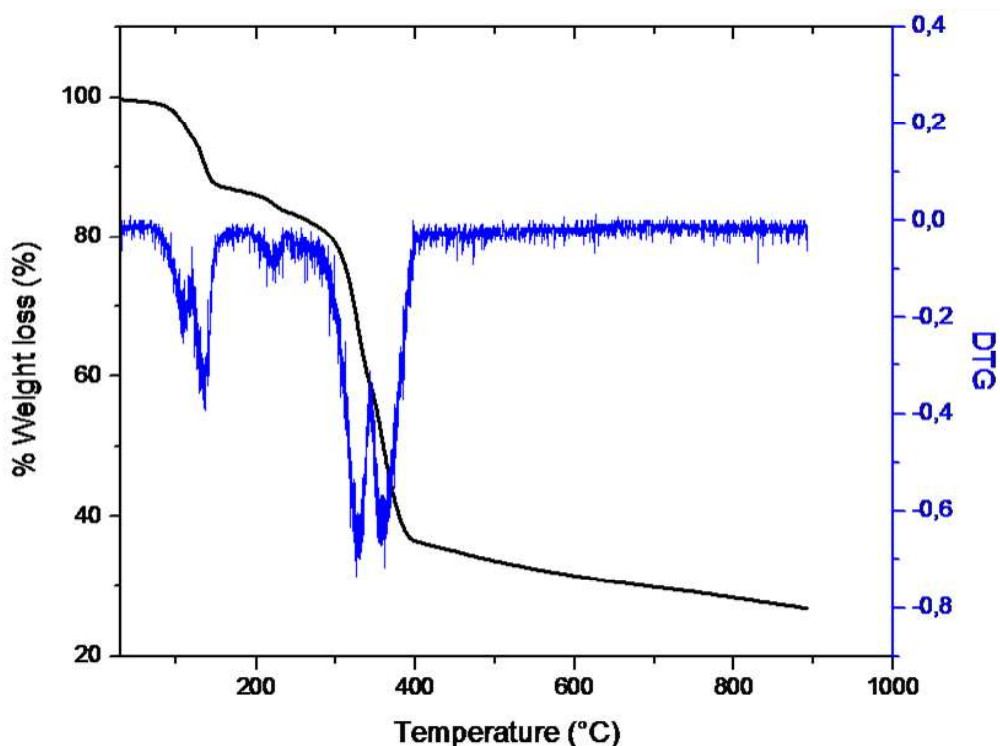
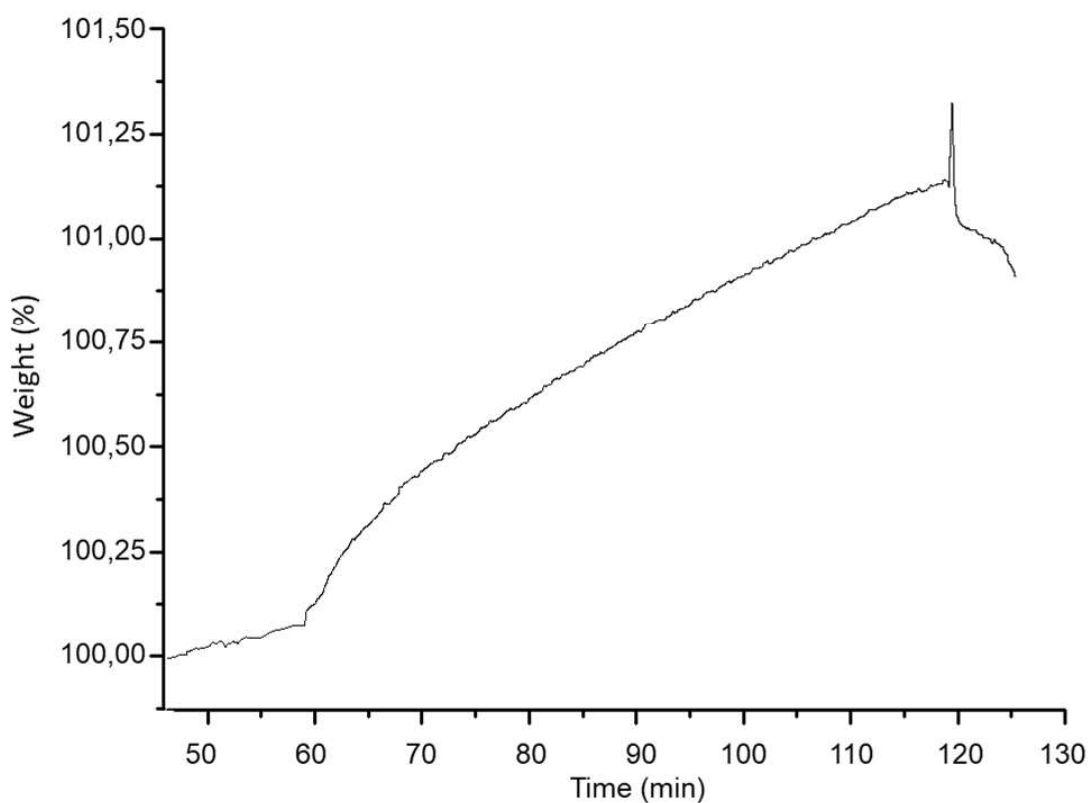


Figure 26. TG/DTG of Cu-BTC synthesized sample

### 5.3.5 CO<sub>2</sub> uptake evaluation

Figure 27 presents the CO<sub>2</sub> adsorption–desorption standard thermogravimetric test for 1.8:1 Cu:BTC sample at 30 °C adsorption and 100 °C desorption. The adsorption experiments were carried out at a temperature of 30 °C under pure CO<sub>2</sub> for 60 min; then, CO<sub>2</sub> was desorbed at 100 °C under pure N<sub>2</sub> for 60 min. The adsorbent loss weight was applied to determine the adsorption and desorption performance of the sample, as used by authors<sup>80,81</sup>. The sorption

capacity of 1.8:1 Cu:BTC ratio was around 1,2 %, while the 1:1 Cu:BTC uptake was 0,34 %. As follows from Figure 27, after performing the standard TG test, the sample did not reach its maximum adsorption capacity at the temperature of 30 °C. To evaluate its maximum capacity, it would be interesting to increase the time of exposure of the sample to the CO<sub>2</sub> atmosphere until its saturation. This sample with high concentration (1.8:1 Cu:BTC) attains then an active sorption capacity of CO<sub>2</sub> higher than the low 1:1 Cu:BTC, which is in line with the literature <sup>77</sup>.



**Figure 27. CO<sub>2</sub> adsorption–desorption for 1.8:1 Cu:BTC sample at 30 °C adsorption and 100 °C desorption.**

The sorption/desorption cycles were then repeated 3 times to evaluate the recuperability of the samples, Figure 28. The metal–organic frameworks exhibited relevant regeneration during the course of the entire experiment. The

results show the sorption capacity of the samples remains very high (85% recoverability) in the second cycle and still presents high adsorption capacity in the third consecutive cycle (64% recoverability in relation to the first cycle). The evaluation of the MOFs in the TG analysis confirmed the stability and its adsorbent properties. In addition, this material presents the possibility of using it in subsequent cycles with high adsorption and regeneration capacity, which is essential to practical and prolonged carbon dioxide applications <sup>42</sup>.

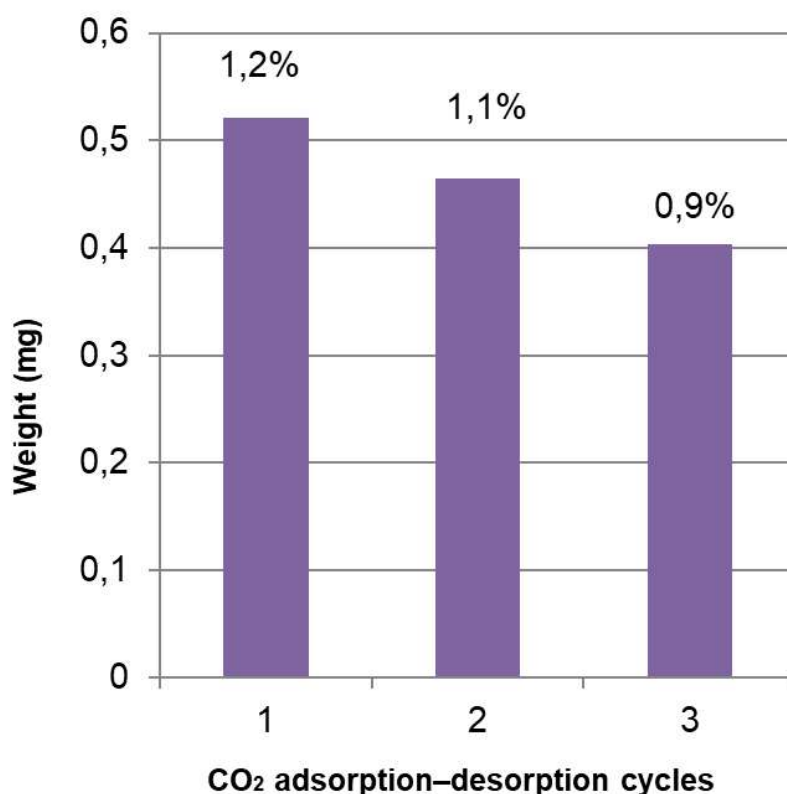


Figure 28. Cycle of CO<sub>2</sub> adsorption-desorption for 1.8:1 Cu:BTC sample at 30 °C adsorption and 100 °C desorption.

#### 5.4 Conclusions

In summary, the obtained results in this study confirmed the successful Cu<sub>3</sub>(BTC)<sub>2</sub> water-based formation. The crystalline MOF can be prepared with excess metal in the synthesis. We observed that the ratio ligand/metal promotes

a remarkable interference in the morphology of final materials. While the low concentration showed ribbons shape, the high ratio of copper (Cu: BTC 1.8:1) provided the building agglomerated granules in well-defined blocks. In conclusion, we obtained a water-based Cu-BTC which has high CO<sub>2</sub> adsorption capacity at room temperature and ambient pressure. Finally, the MOF adsorbent was also found to exhibit repeatability during 3 cycles of adsorption/desorption.

## **CAPÍTULO 6. Considerações finais**

Esta tese de doutorado é a continuidade de um projeto anteriormente desenvolvido pelo autor, enquanto visitava o Instituto de Interfaces Funcionalizadas (IFG) da Universidade de Karlsruhe (KIT), na Alemanha, onde material semelhante foi sintetizado e caracterizado. Nesse sentido, a nova tecnologia foi levada ao Laboratório de Materiais Cerâmicos (LMC/UFGM), juntamente com o aprimoramento dos parâmetros de síntese e avaliação da capacidade desse material quanto à adsorção de gases. Dessa forma, foi realizada uma associação de expertise dos dois laboratórios (LMC/UFGM e IFG/KIT). Essa parceria foi promissora devido à simplicidade da preparação das MOFs obtidas, ao baixo custo de montagem experimental, à excelente infraestrutura do LMC e ao seu histórico em desenvolver novos materiais adsorventes.

Por meio dessa pesquisa foi possível obter SURMOFs homogêneos com alta capacidade de orientação devido ao substrato utilizado. O objetivo principal foi alcançado, por meio do intercâmbio de conhecimentos e do estabelecimento da tecnologia de materiais MOF e SURMOF na UFGM, especialmente no Departamento de Engenharia Metalúrgica e de Materiais. Este trabalho também permitiu a contribuição científica e tecnológica para o desenvolvimento de estruturas organometálicas com novas morfologias e para a fabricação de materiais com potencial para reduzir a emissão de gases poluentes. Novas estruturas foram obtidas, por meio de rotas inovadoras e eficientes, além da caracterização e estudo aprofundado.

Os novos MOFs particulados obtidos através deste trabalho, juntamente com as superfícies modificadas através do crescimento de MOFs apresentam, além da aplicação em adsorção e separação de gases, um amplo espectro de aplicações, como catálise; sensores; dispositivos biomédicos. Associados à recente descoberta de MOFs, isso demonstra a relevância do tema apresentado e a importância de melhorar os métodos de síntese para descobrir novas rotas e mais otimizadas.



## **CHAPTER 6. Final Considerations**

This doctoral thesis is the continuity of a project previously developed by the author while visiting the Institute of Functionalized Interfaces (IFG) at the University of Karlsruhe (KIT), in Germany, where similar material was synthesized and characterized. In this sense, the new technology was brought to the Laboratory Ceramic Materials (LMC/UFMG), together with the improving of the synthesis parameters and evaluate the capacity of this material in gas adsorption. All of this in order to associate the expertise of the two laboratories (LMC/UFMG and IFG/KIT). This partnership was promising due to the simplicity of preparing the MOFs, to the low cost of assembly, to the excellent infrastructure of the LMC and its history regarding the development of new adsorbent materials.

The film of MOF materials, for example, has the property of gas separation <sup>47</sup> and has a relatively low manufacturing cost to provide for large-scale use. It is interesting that the coating has adherence to the substrate in order to provide durability and resistance to possible aggressions related to the environment in which it will be exposed. In this sense, studies on this topic can bring relevant findings.

Through this research it was possible to obtain homogeneous SURMOFs with high orientation capacity due to the chosen substrate. The main objective was achieved through the exchange of knowledge and the establishment of MOF and SURMOF materials technology at UFMG, especially in the Department of Metallurgical and Materials Engineering.

This work also allowed the scientific and technological contribution to the development of new organometallic structures and to the manufacture of materials with the potential to reduce the emission of polluting gases. New

structures were obtained, through innovative and efficient routes, in addition to characterization and in-depth study.

The new particulate MOFs obtained through this work, together with the surfaces modified through the growth of MOFs, in addition to the application in adsorption and gas separation, also have great potential for catalysis; sensors; biomedical devices; drug delivery. This wide spectrum of applications, associated with the recent discovery of MOFs, demonstrates the relevance of the presented theme and the importance of improving synthesis methods in order to discover new and more optimized routes, and original products.

MOFs are famous for their high adsorption capacity. As suggestions for future work, it is interesting to develop a cycle with adequate temperature and time for this material to better explore the potential Cu-BTC MOF can offer. The results shown in this study may seem, at first glance, narrow. However, the CO<sub>2</sub> adsorption capacity and selectivity of MOFs have been found in the literature to be low at atmospheric pressure because of weak interactions between framework and CO<sub>2</sub> gas<sup>82</sup>. The adsorption tests here were carried out at room pressure and room temperatures. Under more aggressive conditions, the adsorption capacity is certainly greater.

## REFERENCES

1. Gascon, J. & Kapteijn, F. Metal-organic framework membranes-high potential, bright future? *Angew. Chemie - Int. Ed.* **49**, 1530–1532 (2010).
2. Vishwakarma, N. K. *et al.* gas / liquid flow. *Nat. Publ. Gr.* **8**, 1–8 (2017).
3. Fischer, R. A. & Bétard, A. Metal-organic framework thin films: From fundamentals to applications. *Chem. Rev.* 1055–1083 (2011).
4. Reza, A., Karimi, M. & Yaser, M. Colloids and Surfaces A : Physicochemical and Engineering Aspects Effect of construction method and surface area for nano metal – organic framework HKUST-1 upon adsorption and removal of phenazopyridine hydrochloride. *Colloids Surfaces A Physicochem. Eng. Asp.* **520**, 193–200 (2017).
5. Tranchemontagne, D. J., Hunt, J. R. & Yaghi, O. M. Room temperature synthesis of metal-organic frameworks: MOF-5, MOF-74, MOF-177, MOF-199, and IRMOF-0. *Tetrahedron* **64**, 8553–8557 (2008).
6. Valadez Sánchez, E. P. *et al.*  $\alpha$ -Al<sub>2</sub>O<sub>3</sub>-supported ZIF-8 SURMOF membranes: Diffusion mechanism of ethene/ethane mixtures and gas separation performance. *J. Memb. Sci.* **594**, 117421 (2020).
7. Gliemann, H. & Wöll, C. Epitaxially grown metal-organic frameworks. *Mater. Today* **15**, 110–116 (2012).
8. Chen, C. *et al.* Synthesis of Hierarchically Structured Hybrid Materials by Controlled Self-Assembly of Metal-Organic Framework with Mesoporous Silica for CO<sub>2</sub> Adsorption. *ACS Appl. Mater. Interfaces* **9**, 23060–23071 (2017).
9. Trickett, C. A. *et al.* The chemistry of metal-organic frameworks for CO<sub>2</sub> capture, regeneration and conversion. *Nat. Rev. Mater.* **2**, 1–16 (2017).
10. Rowsell, J. L. C. & Yaghi, O. M. Metal-organic frameworks: A new class

- of porous materials. *Microporous Mesoporous Mater.* **73**, 3–14 (2004).
11. Dantas Ramos, A. L., Tanase, S. & Rothenberg, G. Redes metalorgânicas e suas aplicações em catálise. *Quim. Nova* **37**, 123–133 (2014).
  12. Aguado, S. *et al.* Facile synthesis of an ultramicroporous MOF tubular membrane with selectivity towards CO<sub>2</sub>. *New J. Chem.* **35**, 41–44 (2011).
  13. Hailian Li\*, Mohamed Eddaoudi<sup>2</sup>, M. O. & O. M. Y. Design and synthesis of an exceptionally stable and highly MOF. *Nature* **402**, 276–279 (1999).
  14. Bétard, A. *et al.* Fabrication of a CO<sub>2</sub>-selective membrane by stepwise liquid-phase deposition of an alkylether functionalized pillared-layered metal-organic framework [Cu<sub>2</sub>L<sub>2</sub>P]<sub>n</sub> on a macroporous support. *Microporous Mesoporous Mater.* **150**, 76–82 (2012).
  15. Best, J. P. *et al.* Nanomechanical investigation of thin-film electroceramic/metal-organic framework multilayers. *Appl. Phys. Lett.* **107**, (2015).
  16. Alduhaish, O. *et al.* A two-dimensional microporous metal–organic framework for highly selective adsorption of carbon dioxide and acetylene. *Chinese Chem. Lett.* **28**, 1653–1658 (2017).
  17. Brant, J. A., Liu, Y., Sava, D. F., Beauchamp, D. & Eddaoudi, M. Single-metal-ion-based molecular building blocks (MBBs) approach to the design and synthesis of metal-organic assemblies. *J. Mol. Struct.* **796**, 160–164 (2006).
  18. Kalmutzki, M. J., Hanikel, N. & Yaghi, O. M. Secondary building units as the turning point in the development of the reticular chemistry of MOFs. *Sci. Adv.* **4**, (2018).
  19. Almeida Paz, F. A. *et al.* Ligand design for functional metal-organic frameworks. *Chem. Soc. Rev.* **41**, 1088–1110 (2012).

20. Meek, S. T., Greathouse, J. A. & Allendorf, M. D. Metal-organic frameworks: A rapidly growing class of versatile nanoporous materials. *Adv. Mater.* **23**, 249–267 (2011).
21. Schlichte, K., Kratzke, T. & Kaskel, S. Improved synthesis, thermal stability and catalytic properties of the metal-organic framework compound Cu<sub>3</sub>(BTC)<sub>2</sub>. *Microporous Mesoporous Mater.* **73**, 81–88 (2004).
22. Duan, J., Pan, Y., Liu, G. & Jin, W. Metal-organic framework adsorbents and membranes for separation applications. *Curr. Opin. Chem. Eng.* **20**, 122–131 (2018).
23. He, H., Perman, J. A., Zhu, G. & Ma, S. Metal-Organic Frameworks for CO<sub>2</sub> Chemical Transformations. *Small* **12**, 6309–6324 (2016).
24. Choi, K. M. *et al.* Plasmon-enhanced photocatalytic CO<sub>2</sub> conversion within metal-organic frameworks under visible light. *J. Am. Chem. Soc.* **139**, 356–362 (2017).
25. Lin, W. *et al.* A porous Zn-based metal-organic framework for pH and temperature dual-responsive controlled drug release. *Microporous Mesoporous Mater.* **249**, 55–60 (2017).
26. Stock, N. & Biswas, S. Synthesis of metal-organic frameworks (MOFs): Routes to various MOF topologies, morphologies, and composites. *Chem. Rev.* **112**, 933–969 (2012).
27. Liu, J. *et al.* Deposition of metal-organic frameworks by liquid-phase epitaxy: The influence of substrate functional group density on film orientation. *Materials (Basel)*. **5**, 1581–1592 (2012).
28. Kind, M. & Wöll, C. Organic surfaces exposed by self-assembled organothiol monolayers: Preparation, characterization, and application. *Prog. Surf. Sci.* **84**, 230–278 (2009).

29. Liu, J. *et al.* Structural characterization of self-assembled monolayers of pyridine-terminated thiolates on gold. *Phys. Chem. Chem. Phys.* **12**, 4459–4472 (2010).
30. Cesarino, I., Marino, G., Matos, J. D. R. & Cavaleiro, É. T. G. Using the organofunctionalised SBA-15 nanostructured silica as a carbon paste electrode modifier: Determination of cadmium ions by differential anodic pulse stripping voltammetry. *J. Braz. Chem. Soc.* **18**, 810–817 (2007).
31. De Magalhães, G. O., de Oliveira Notório Ribeiro, J., Vasconcelos, D. C. L. & Vasconcelosa, W. L. Production of pure granules of SBA-15 mesoporous silica. *Mater. Res.* **21**, (2018).
32. Shekhah, O., Wang, H., Zacher, D., Fischer, R. A. & Wöll, C. Growth mechanism of metal-organic frameworks: Insights into the nucleation by employing a step-by-step route. *Angew. Chemie - Int. Ed.* **48**, 5038–5041 (2009).
33. Arslan, H. K. *et al.* High-throughput fabrication of uniform and homogenous MOF coatings. *Adv. Funct. Mater.* **21**, 4228–4231 (2011).
34. Bradshaw, D., Garai, A. & Huo, J. Metal-organic framework growth at functional interfaces: Thin films and composites for diverse applications. *Chem. Soc. Rev.* **41**, 2344–2381 (2012).
35. Horike, S., Dincă, M., Tamaki, K. & Long, J. R. Size-selective Lewis acid catalysis in a microporous metal-organic framework with exposed Mn<sup>2+</sup> coordination sites. *J. Am. Chem. Soc.* **130**, 5854–5855 (2008).
36. Motakef-Kazemi, N., Shojaosadati, S. A. & Morsali, A. In situ synthesis of a drug-loaded MOF at room temperature. *Microporous Mesoporous Mater.* **186**, 73–79 (2014).
37. Mamleyev, E. R. *et al.* Laser-induced hierarchical carbon patterns on polyimide substrates for flexible urea sensors. *npj Flex. Electron.* **3**, (2019).

38. Gulati, P., Lindemann, L., Heinke, J., Liu, M., Tsotsalas, C., Wöll, H. G. Surface-Anchored Metal-Organic Frameworks – SURMOFs: A New Material Platform for Sensors. *12. Dresdner Sensor-Symposium 2015* 234–238 (2015) doi:10.5162/12dss2015/P7.6.
39. Zhao, X., Wang, Y., Li, D. S., Bu, X. & Feng, P. Metal–Organic Frameworks for Separation. *Adv. Mater.* **30**, 1–34 (2018).
40. Lim, S. Y. *et al.* New CO<sub>2</sub> separation membranes containing gas-selective Cu-MOFs. *J. Memb. Sci.* **467**, 67–72 (2014).
41. Wriedt, M., Sculley, J. P., Verdegaal, W. M., Yakovenko, A. A. & Zhou, H. C. Unprecedented activation and CO<sub>2</sub> capture properties of an elastic single-molecule trap. *Chem. Commun.* **49**, 9612–9614 (2013).
42. Sumida, K. *et al.* Carbon dioxide capture in metal-organic frameworks. *Chem. Rev.* **112**, 724–781 (2012).
43. Argoub, A. *et al.* Synthesis of MIL-101@g-C<sub>3</sub>N<sub>4</sub> nanocomposite for enhanced adsorption capacity towards CO<sub>2</sub>. *J. Porous Mater.* **25**, 1–7 (2017).
44. Liang, Z., Marshall, M. & Chaffee, A. L. CO<sub>2</sub> adsorption-based separation by metal organic framework (Cu-BTC) versus zeolite (13X). *Energy and Fuels* **23**, 2785–2789 (2009).
45. Domán, A., Madarász, J. & László, K. In situ evolved gas analysis assisted thermogravimetric (TG-FTIR and TG/DTA–MS) studies on non-activated copper benzene-1,3,5-tricarboxylate. *Thermochim. Acta* **647**, 62–69 (2017).
46. Derakhshani, M., Hashamzadeh, A. & Amini, M. M. Novel synthesis of mesoporous crystalline  $\gamma$ -alumina by replication of MOF-5-derived nanoporous carbon template. *Ceram. Int.* **44**, 17102–17106 (2018).
47. Liu, Y. *et al.* Synthesis of continuous MOF-5 membranes on porous  $\alpha$ -

- alumina substrates. *Microporous Mesoporous Mater.* **118**, 296–301 (2009).
48. Furukawa, H., Cordova, K. E., O’Keeffe, M. & Yaghi, O. M. The chemistry and applications of metal-organic frameworks. *Science* (2013) doi:10.1126/science.1230444.
  49. Liu, J. & Wöll, C. Surface-supported metal-organic framework thin films: Fabrication methods, applications, and challenges. *Chem. Soc. Rev.* **46**, 5730–5770 (2017).
  50. Fu, L. *et al.* Synthesis and carbon dioxide sorption of layered double hydroxide/silica foam nanocomposites with hierarchical mesostructure. *ChemSusChem* **7**, 1035–1039 (2014).
  51. Shekhah, O. *et al.* Successful implementation of the stepwise layer-by-layer growth of MOF thin films on confined surfaces: Mesoporous silica foam as a first case study. *Chem. Commun.* **48**, 11434–11436 (2012).
  52. McCarthy, B. D., Liseev, T., Beiler, A. M., Materna, K. L. & Ott, S. Facile Orientational Control of M2L2P SURMOFs on Silicon Substrates and Growth Mechanism Insights for Defective MOFs. *ACS Appl. Mater. Interfaces* **11**, 38294–38302 (2019).
  53. Wu, C. M., Rathi, M., Ahrenkiel, S. P., Koodali, R. T. & Wang, Z. Facile synthesis of MOF-5 confined in SBA-15 hybrid material with enhanced hydrostability. *Chem. Commun.* **49**, 1223–1225 (2013).
  54. Ribeiro, J. de O. N., Vasconcelos, D. C. L. & Vasconcelos, W. L. Importance of the Order of Addition of the Alumina Precursor and its Type Into Al-SBA-15 Mesoporous Materials for Use as Water Adsorbents. *Mater. Res.* **22**, 1–8 (2018).
  55. de O. N. Ribeiro, J. *et al.* Role of the type of grafting solvent and its removal process on APTES functionalization onto SBA-15 silica for CO<sub>2</sub> adsorption. *J. Porous Mater.* **26**, 1581–1591 (2019).



56. Zhuravlev, L. T. The surface chemistry of amorphous silica. Zhuravlev model. *Colloids Surfaces A Physicochem. Eng. Asp.* **173**, 1–38 (2000).
57. Hermes, S., Zacher, D., Baunemann, A., Wöll, C. & Fischer, R. A. Selective growth and MOCVD loading of small single crystals of MOF-5 at alumina and silica surfaces modified with organic self-assembled monolayers. *Chem. Mater.* **19**, 2168–2173 (2007).
58. Shan, M. *et al.* Facile manufacture of porous organic framework membranes for precombustion CO<sub>2</sub> capture. *Sci. Adv.* **4**, 1–7 (2018).
59. Remya, V. R. & Kurian, M. Synthesis and catalytic applications of metal–organic frameworks: a review on recent literature. *Int. Nano Lett.* **9**, 17–29 (2019).
60. Kayal, S., Chakraborty, A. & Teo, H. W. B. Green synthesis and characterization of aluminium fumarate metal-organic framework for heat transformation applications. *Mater. Lett.* **221**, 165–167 (2018).
61. Chen, T. *et al.* A novel hexagonal prism Cu-BTC by unipolar pulse electropolymerization. *Mater. Lett.* **254**, 137–140 (2019).
62. Moosavi, S. M. *et al.* Capturing chemical intuition in synthesis of metal-organic frameworks. *Nat. Commun.* **10**, 1–7 (2019).
63. Li, Z. Q. *et al.* Ultrasonic synthesis of the microporous metal-organic framework Cu<sub>3</sub>(BTC)<sub>2</sub> at ambient temperature and pressure: An efficient and environmentally friendly method. *Mater. Lett.* **63**, 78–80 (2009).
64. Xu, H., Zeiger, B. W. & Suslick, K. S. Sonochemical synthesis of nanomaterials. *Chem. Soc. Rev.* **42**, 2555–2567 (2013).
65. Sargazi, G., Afzali, D., Ghafainazari, A. & Saravani, H. Rapid Synthesis of Cobalt Metal Organic Framework. *J. Inorg. Organomet. Polym. Mater.* **24**, 786–790 (2014).

66. da Silva, G. G. *et al.* Sonoelectrochemical synthesis of metal-organic frameworks. *Synth. Met.* **220**, 369–373 (2016).
67. Israr, F. *et al.* Synthesis of porous Cu-BTC with ultrasonic treatment: Effects of ultrasonic power and solvent condition. *Ultrason. Sonochem.* **29**, 186–193 (2016).
68. Luo, Y., Chen, D., Wei, F. & Liang, Z. Synthesis of Cu-BTC Metal-Organic Framework by Ultrasonic Wave-Assisted Ball Milling with Enhanced Congo Red Removal Property. *ChemistrySelect* **3**, 11435–11440 (2018).
69. Dhumal, N. R., Singh, M. P., Anderson, J. A., Kiefer, J. & Kim, H. J. Molecular Interactions of a Cu-Based Metal-Organic Framework with a Confined Imidazolium-Based Ionic Liquid: A Combined Density Functional Theory and Experimental Vibrational Spectroscopy Study. *J. Phys. Chem. C* **120**, 3295–3304 (2016).
70. G.K. Williamson and W.H. Hall. X-ray line broadening from fcc aluminium and Wolfram. *Acta Metall.* **1**, 22–31 (1953).
71. Chui, S. S. Y., Lo, S. M. F., Charmant, J. P. H., Orpen, A. G. & Williams, I. D. A chemically functionalizable nanoporous material [Cu<sub>3</sub>(TMA)<sub>2</sub>(H<sub>2</sub>O)<sub>3</sub>]<sub>n</sub>. *Science* (80-. ). **283**, 1148–1150 (1999).
72. Liao, P. *et al.* Transforming HKUST-1 Metal–Organic Frameworks into Gels – Stimuli-Responsiveness and Morphology Evolution. *Eur. J. Inorg. Chem.* **2017**, 2580–2584 (2017).
73. Furukawa, S. S. D. Controlled Multiscale Synthesis of Porous Coordination Polymer in Nano/Micro Regimes. *Chem. Mater.* **22**, 4531–4538 (2010).
74. Wang, Z., Weidler, P. G., Azucena, C., Heinke, L. & Wöll, C. Negative, anisotropic thermal expansion in monolithic thin films of crystalline metal-organic frameworks. *Microporous Mesoporous Mater.* **222**, 241–246 (2016).

75. Wang, Z. *et al.* Resistive switching nanodevices based on metal–organic frameworks. *ChemNanoMat* **2**, 67–73 (2016).
76. Saha, D. & Deng, S. Hydrogen Adsorption on Metal-Organic Framework MOF-177. **15**, 363–376 (2010).
77. Pereira da Silva, C. T. *et al.* Synthesis of Zn-BTC metal organic framework assisted by a home microwave oven and their unusual morphologies. *Mater. Lett.* **182**, 231–234 (2016).
78. Gascon, J., Aguado, S. & Kapteijn, F. Manufacture of dense coatings of Cu<sub>3</sub>(BTC)<sub>2</sub> (HKUST-1) on  $\alpha$ -alumina. *Microporous Mesoporous Mater.* **113**, 132–138 (2008).
79. Mengyu Ma, Liangyu Lu, Hongwei Li, Y. X. and F. D. \*. Functional Metal Organic Framework / SiO<sub>2</sub> Nanocomposites : From Versatile Synthesis to. *Polym. Appl. Adv.* (2019).
80. Kapica-Kozar, J. *et al.* Titanium dioxide modified with various amines used as sorbents of carbon dioxide. *New J. Chem.* **41**, 1549–1557 (2017).
81. Majchrzak-Kucęba, I. & Bukalak-Gaik, D. Regeneration performance of metal–organic frameworks: TG-Vacuum tests. *J. Therm. Anal. Calorim.* **125**, 1461–1466 (2016).
82. Yan, X., Komarneni, S., Zhang, Z. & Yan, Z. Extremely enhanced CO<sub>2</sub> uptake by HKUST-1 metal-organic framework via a simple chemical treatment. *Microporous Mesoporous Mater.* **183**, 69–73 (2014).